

Development of load-resistance-factor-design-based prestressed concrete tub girders in Colorado

Yail J. Kim and Jun Wang

- This paper explores the development of new prestressed concrete tub girders for use in Colorado to surpass the performance of currently used girders.
- For comparison, 35 existing girder types were reviewed from six transportation agencies across the United States.
- To comprehend the practicality of the prototype girders, five bridge superstructures were designed and their behavior was studied. In addition, the estimated production costs and monetary benefits were reviewed for the prototype girders.

Trends in modern bridge construction include light weight, extended longevity, long spans, cost-effectiveness, and specific aesthetics.¹ Particularly, the demands for controlled quality, prompt erection, affordable maintenance, and larger span-to-depth ratios are escalating in highway bridges across metropolitan areas where topographical constraints and traffic disruptions bring significant challenges. Prestressed concrete offers competitive solutions that accommodate these requirements. For example, the shallow depth of prestressed concrete girders lessens the dead load, material consumption, and overall budget of a bridge system;² in addition, transported girders may be spliced on-site to provide structural continuity so that statical indeterminacy becomes available, which is beneficial in terms of reducing deflections and stresses under vehicular loadings.

On the grounds of these merits, a variety of girder types have been produced and technical endeavors continued to advance the state of the art.³ Bardow et al.⁴ discussed a case study that addressed disparities between local design standards and actual practices. A committee comprising both public and private sector members deliberated an upgrade of prestressed concrete girders. Under consideration were spatial restrictions, handling and erection, regional environments, and alignment with widening roads. Third parties independently reviewed finalized prototypes to reaffirm the feasibility of the sections. Seguirant⁵ presented a girder series to supersede the Washington Department of Transportation standards. The depth of the series was 129% greater than that

of the existing sections in order to increase the span length of continuous bridges and the spacing between adjacent girders. The thickness of the web was 6.1 and 7.87 in. (155 and 200 mm) for pretensioning and post-tensioning applications, respectively. The wide flanges of the girders elevated lateral stability during shipping. Hovell et al.⁶ reported detailing improvements for the end region of prestressed girders. Various specimens were monotonically loaded with straight and angled geometries. The customary reinforcing schemes of the Texas Department of Transportation were revised with extra steel bars in the flange and the webs. Standard design was then suggested to place auxiliary stirrups and confining reinforcing bars and to expand the size of end blocks. Amir and Shakour⁷ attempted to figure out efficient tendon layouts in simply supported prestressed concrete beams. Relying on the magnitudes of self-weight and external loads, principal stresses evolved and, thus, tendon arrangements were updated to generate a concordant profile. Supplementary research was recommended to ascertain interactions between multiple tendons.

Among others, tub girders have received special attention because they play an important role in the structural response of slab-on-girder bridges and construction costs.⁸ Tub girders are defined as open-section trapezoidal elements with narrow and inclined webs. From a functionality standpoint, such girders have aesthetic appeal, adaptability to straight and horizontally curved superstructures, favorable stiffness, and convenient shipping and handling.

Several projects are noteworthy in the development and appraisal of prestressed concrete tub girders. Ralls et al.⁹ proposed alternative tub girders with the intention of substituting I-shaped girders in Texas, which require close spacing and are not aesthetically pleasing. The efficiency of the proposed tub girders was compared against those of equivalent I-shaped girders. Huang and Shahawy¹⁰ carried out finite element modeling to predict stress levels along tub girders under service loading. Stress concentrations were observed near the corners where the bottom flange and webs were integrated, leading to the onset of end zone cracking. Reese¹¹ collected case studies on the subject of tub girders in Colorado. Emphasis was placed on splicing precast concrete members and erect-

ing segments in complex site conditions. Properly planned girder lengths reduced the need to use temporary shoring and facilitated longitudinal prestressing operations. Optimization techniques also guided researchers to find solutions that can minimize costs while maintaining adequate capacities in prestressed concrete tub girders.^{12,13}

In consonance with the knowledge accumulated over decades, transportation agencies select standard tub girders and deploy them for bridge projects. It should, however, be noted that there is no consensus on the format of these girders and individual agencies prefer certain shapes and strand placements. Consequently, state departments of transportation are ultimately responsible for managing, upgrading, and replacing existing girders in order to warrant the best infrastructure options and are continually seeking opportunities that satisfy intended goals. As part of such efforts, a research program is presented in this paper, and its three objectives are as follows:

- to develop optimized tub girder sections that can surpass the performance of girders currently used in Colorado
- to evaluate the behavior of bridge structures incorporating the new sections against the prescriptive articles of the American Association of State Highway and Transportation Officials' *AASHTO LRFD Bridge Design Specifications*¹⁴
- to suggest an implementable girder series for practice

Evaluation of existing tub girders

Geometric properties

Figure 1 shows archetypal tub girders used by state departments of transportation in the United States. While all girders are composed of upper and lower flanges and inclined webs, specific configurations vary by state. For example, the inner side of the upper flanges in the Texas and Colorado girders is flat; on the other hand, the Washington girder has protruded upper flanges. For comparison, multiple variables were assigned to each segment of the girders (Fig. 1) and summarized in Table 1, where 35 types are detailed. The depth of these

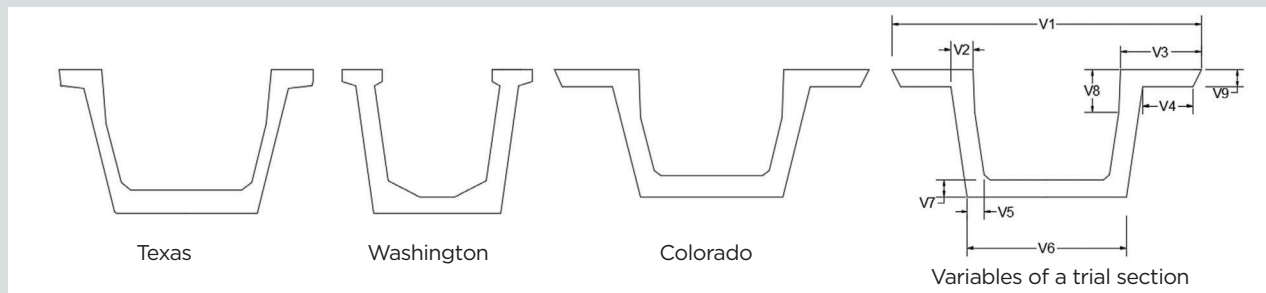


Figure 1 Geometric configuration of tub girders. Note: V_1 = upper girder width; V_2 = upper web thickness; V_3 = flange length; V_4 = flange extension; V_5 = lower web thickness; V_6 = bottom girder width; V_7 = bottom flange thickness; V_8 = depth to web angle; V_9 = upper flange thickness.

Table 1. Geometric variable of existing tub girders

State/agency	Girder type	Depth, in.	V_1 , in.	V_2 , in.	V_3 , in.	V_4 , in.	V_5 , in.	V_6 , in.	V_7 , in.	V_8 , in.	V_9 , in.	n	t_{web} , in.
California DOT	UB1400	55	86.6	7.9	13.8	8.9	7.9	59.1	6.9	11.8	11.8	3.1	7.9
	UB 550	61	89.6	7.9	15.3	8.9	7.9	59.1	6.9	11.8	11.8	3.2	7.9
	UB1700	67	92.5	7.9	16.7	8.9	7.9	59.1	6.9	11.8	11.8	3.3	7.9
	UB1850	73	95.5	7.9	18.2	8.9	7.9	59.1	6.9	11.8	11.8	3.4	7.9
	UB2000	79	98.4	7.9	19.7	8.9	7.9	59.1	6.9	11.8	11.8	3.4	7.9
	UB2150	85	101.4	7.9	21.2	8.9	7.9	59.1	6.9	11.8	11.8	3.4	7.9
Colorado DOT	U48	48	115	10	30	16.8	5.2	54	8.1	18	6.4	4	7.5
	U60	60	121	10	30	16.8	5.2	54	8.1	18	6.4	4	7.5
	U72	72	127	10	30	16.8	5.2	54	8.1	18	6.4	4	7.5
	U84	84	133	10	30	16.8	5.2	54	8.1	18	6.4	4	7.5
	U96	96	139	10	30	16.8	5.2	54	8.1	18	6.4	4	7.5
Florida DOT	FU48	48	94	6.6	16	8.5	n/a	56	10	21	7	4	5.5
	FU54	54	97	6.6	16	8.5	n/a	56	10	21	7	4	5.5
	FU63	63	102	6.6	16	8.5	n/a	56	10	21	7	4	5.5
	FU72	72	106	6.6	16	8.5	n/a	56	10	21	7	4	5.5
PCI	PCI72_9	72	121	10.3	20	7.5	n/a	70	9	21	9.3	4	9
	PCI84_9	84	127	10.3	20	7.5	n/a	70	9	21	9.3	4	9
	PCI96_9	96	133	10.3	20	7.5	n/a	70	9	21	9.3	4	9
	PCI72_10	72	123	11.3	21	7.5	n/a	72	9	21	9.3	4	10
	PCI84_10	84	129	11.3	21	7.5	n/a	72	9	21	9.3	4	10
	PCI96_10	96	135	11.3	21	7.5	n/a	72	9	21	9.3	4	10
Texas DOT	U 40	40	89	7.5	15.8	8.3	n/a	55	8.3	21.6	5.9	4	5
	U 54	54	96	7.5	15.8	8.3	n/a	55	8.3	21.6	5.9	4	5
	U72_9	72	121	10.3	20	7.5	n/a	70	9	21	9.3	4	9
	U84_9	84	127	10.3	20	7.5	n/a	70	9	21	9.3	4	9
	U96_9	96	133	10.3	20	7.5	n/a	70	9	21	9.3	4	9
	U72_10	72	123	11.3	21	7.5	n/a	72	9	21	9.3	4	10
	U84_10	84	129	11.3	21	7.5	n/a	72	9	21	9.3	4	10
	U96_10	96	135	11.3	21	7.5	n/a	72	9	21	9.3	4	10
Washington DOT	U54_4	54	71.7	7.1	15.1	5.0	n/a	48	6	n/a	4.5	7	7
	U66_4	66	75.1	7.1	15.1	5.0	n/a	48	6	n/a	4.5	7	7
	U78_4	78	78.6	7.1	15.1	5.0	n/a	48	6	n/a	4.5	7	7
	U54_5	54	83.7	7.1	15.1	5.0	n/a	60	6	n/a	4.5	7	7
	U66_5	66	87.1	7.1	15.1	5.0	n/a	60	6	n/a	4.5	7	7
	U78_5	78	90.6	7.1	15.1	5.0	n/a	60	6	n/a	4.5	7	7

Note: DOT = department of transportation; n = slope of web; n/a = not applicable; t_{web} = thickness of web.

Table 2. Structural efficiency of existing tub girders

State/agency	Girder type	Depth, in.	Efficiency factor ρ	Efficiency ratio α	Weight, kip/ft
California DOT	UB1400	55	0.46	0.90	1.39
	UB1550	61	0.46	0.89	1.49
	UB1700	67	0.46	0.88	1.59
	UB1850	73	0.45	0.87	1.69
	UB2000	79	0.45	0.86	1.79
	UB2150	85	0.45	0.85	1.89
Colorado DOT	U48	48	0.50	0.89	1.43
	U60	60	0.50	0.89	1.62
	U72	72	0.50	0.88	1.81
	U84	84	0.49	0.86	2.01
	U96	96	0.48	0.85	2.20
Florida DOT	FU48	48	0.48	0.99	1.26
	FU54	54	0.49	1.00	1.33
	FU63	63	0.50	1.01	1.43
	FU72	72	0.50	1.01	1.54
PCI	PCI72_9	72	0.48	0.92	2.12
	PCI84_9	84	0.47	0.90	2.35
	PCI96_9	96	0.47	0.88	2.59
	PCI72_10	72	0.47	0.89	2.28
	PCI84_10	84	0.46	0.87	2.53
	PCI96_10	96	0.46	0.86	2.79
Texas DOT	U 40	40	0.48	0.99	1.02
	U 54	54	0.51	1.03	1.17
	U72_9	72	0.48	0.91	2.12
	U84_9	84	0.47	0.90	2.35
	U96_9	96	0.47	0.88	2.59
	U72_10	72	0.47	0.89	2.28
	U84_10	84	0.46	0.87	2.53
	U96_10	96	0.46	0.86	2.79
Washington DOT	U54_4	54	0.41	0.86	1.08
	U66_4	66	0.41	0.85	1.26
	U78_4	78	0.41	0.83	1.44
	U54_5	54	0.42	0.93	1.16
	U66_5	66	0.42	0.90	1.33
	U78_5	78	0.42	0.88	1.51

Note: DOT = department of transportation.

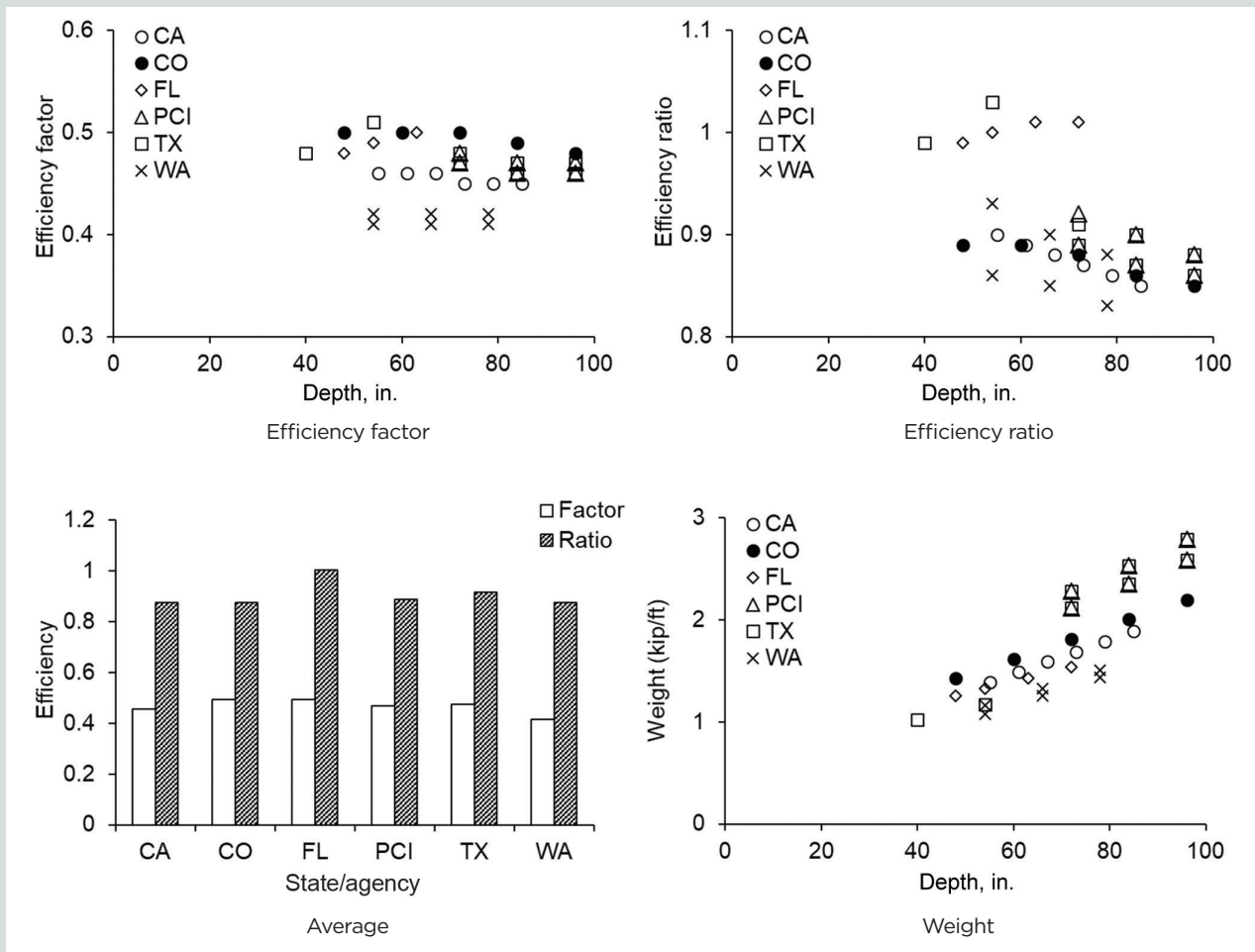


Figure 2. Comparison of efficiency in existing girders. Note: CA = California; CO = Colorado; FL = Florida; TX = Texas; WA = Washington. 1 in. = 25.4 mm; 1 kip/ft = 14.593 kN/m.

existing girders ranged from 40 to 96 in. (1016 to 2438 mm) with a web thickness of 5 to 10 in. (127 to 254 mm), and the radius of gyration r and section moduli S of the girders rose with the increased girder depth. The cross-sectional area A and the moment of inertia I of the Washington girders are in general smaller than those of others because of the compact shape (Fig. 1). The B618 girders employed in Colorado have assorted depths (48, 60, 72, 84, and 96 in. [1219, 1524, 1829, 2134, and 2438 mm] designated as the U48 to U96 girders) with web thicknesses of 5, 7.5, and 10 in. (127, 190.5, and 254 mm) bottom flange thicknesses of 6.35 and 8.1 in. (161 and 206 mm). (A web thickness of 7.5 in. and flange thickness of 8.1 in. were used in Table 1 and the present study unless otherwise stated.) In practice, a bridge system with twin tub girders is often constructed at a deck width varying from 33 to 47 ft (10 to 14 m) with a girder spacing between 12 and 26 ft (4 and 8 m) on center.⁸

Structural efficiency

Analytical approach The prestressed concrete community has adopted the following structural efficiency factor (Eq. [1])

and efficiency ratio (Eq. [2]) to evaluate the geometry of a girder section:¹⁵

$$\rho = \frac{r^2}{y_t y_b} \quad (1)$$

where

ρ = structural efficiency factor

y_t = distance from the centroid of the girder section to the top fiber

y_b = distance from the centroid of the girder section to the bottom fiber

$$\alpha = \frac{3.46S_b}{Ah} \quad (2)$$

where

α = structural efficiency ratio

S_b = section modulus for the bottom fiber

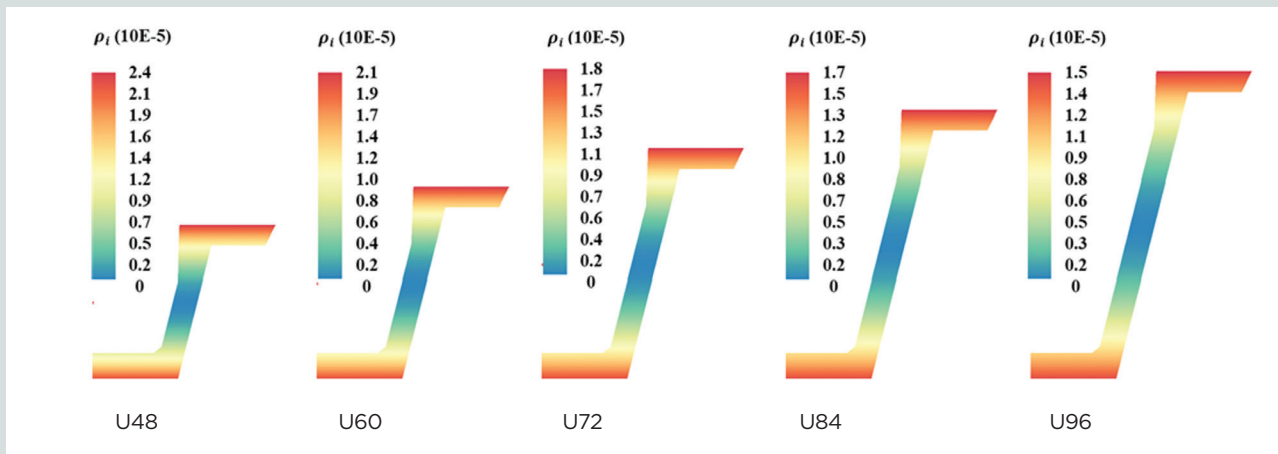


Figure 3. Contribution of geometric components to efficiency factor of B618 girder. Note: ρ_i = efficiency fraction of i th entity in agent-based modeling.

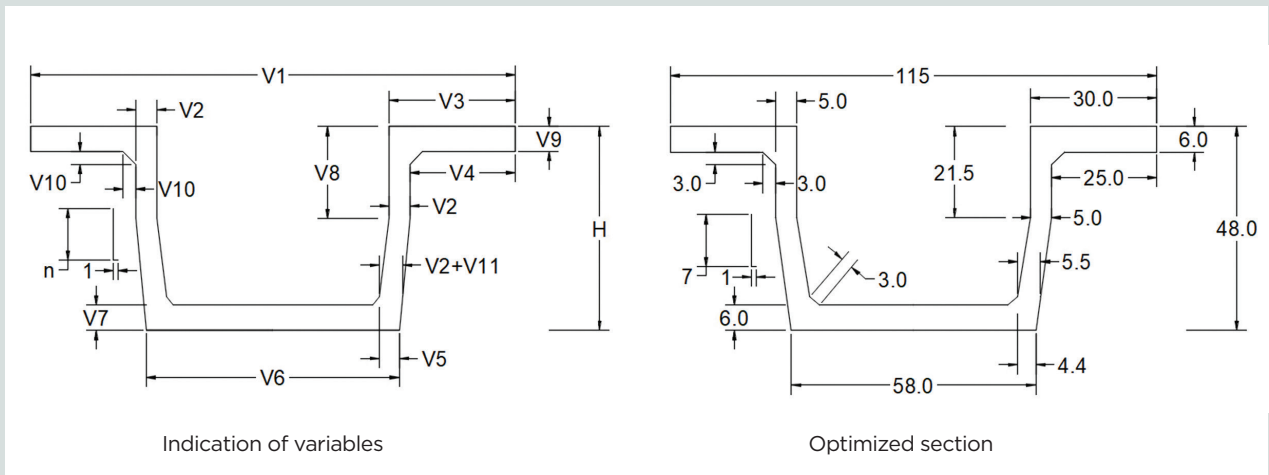


Figure 4. Development of prototype girder. Note: All units are in inches. H = girder depth; n = number of entities covering the girder section in agent-based modeling; slope of girder web; V_1 = upper girder width; V_2 = upper web thickness; V_3 = flange length; V_4 = flange extension; V_5 = lower web thickness; V_6 = bottom girder width; V_7 = bottom flange thickness; V_8 = depth to web angle; V_9 = upper flange thickness; V_{10} = chamfer; V_{11} = web thickness. 1 in. = 25.4 mm.

H = depth of the girder

Listed in **Table 2** are the calculated efficiency factors and ratios of the girders alongside unit weight in kip/ft. Although all structural efficiency factors ρ were within a similar boundary (**Fig. 2**), the factors of the Washington and Texas girders exhibited the lowest and highest values, 0.41 and 0.51, respectively. As far as the structural efficiency ratios α are concerned, the Florida girders, at an average of 1.0, were superior to others demonstrating analogous mean structural efficiency ratio ρ values (**Fig. 2**). The unit weight of the Colorado girders was heavier up to a depth of 60 in. (1524 mm), beyond which the weight of the PCI and Texas girders was noticeable (**Fig. 2**). Given that tub girders span 120 to 160 ft (37 to 49 m),¹⁶ a marginal difference in the unit weight can cause a substantial increase in the dead load of a bridge system. It is,

thus, recommended that the weight of the Colorado girders be reduced to the level of the Florida and Washington girders which have lighter weight and improved structural efficiency.

Computational approach Computational modeling was carried out to investigate the implications of geometric components for structural efficiency of the tub girders (because Eq. [2] contained an empirical constant, Eq. [1] was used). Colorado's B618 series was selected and an open-source cross-platform model called NetLogo¹⁷ was employed. This program utilizes discrete entities in a grid space to simulate their mutual interactions with a preset rule. The principles and implementation procedure of the software are explained in Wilensky and Rand.¹⁷ The size of each entity was determined by sensitivity analysis (0.125×0.125 in. [3.175×3.175 mm]) and the number of the entities varied from 43,762 to 67,474,

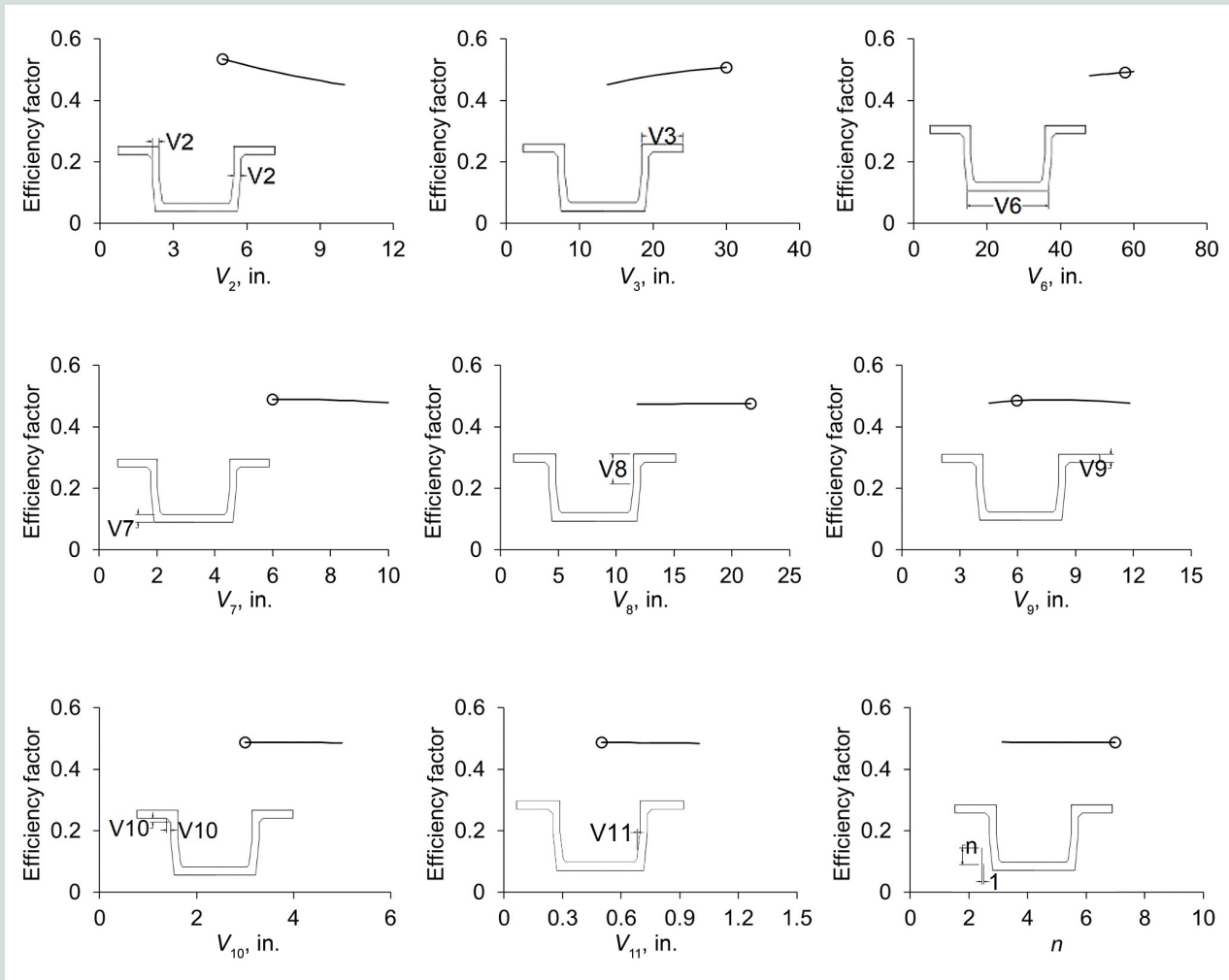


Figure 5. Variation of efficiency factor with geometric properties (where circle is optimized value). Note: n = number of entities covering the girder section in agent-based modeling; slope of girder web; V_2 = upper web thickness; V_3 = flange length; V_6 = bottom girder width; V_7 = bottom flange thickness; V_8 = depth to web angle; V_9 = upper flange thickness; V_{10} = chamfer; V_{11} = lower web thickness. 1 in. = 25.4 mm.

contingent on the girder depth of U48 to U96. The model represented one-half of the symmetric girder section. Aligning with the definition of the efficiency factor ρ , Eq. (3) through (5) were formulated as follows:

$$\rho = \frac{r^2}{y_i y_b} = \frac{I/A}{(h - y_b) y_b} \quad (3)$$

$$A = \sum_{i=1}^n s^2 \quad (4)$$

where

n = number of entities covering the girder section

s = width and depth of the entity

$$I = \sum_{i=1}^n \left(\frac{s^4}{12} + s^2 (y_i - y_b)^2 \right) \quad (5)$$

where

y_i = distance from the bottom of the girder to the centroid of the i th entity

The distance from the neutral axis of the girder to the bottom fiber y_b is expressed as Eq. (6).

$$y_b = \frac{\sum_{i=1}^n s^2 y_i}{\sum_{i=1}^n s^2} \quad (6)$$

Substituting Eq. (4) and (5) into Eq. (3) results in Eq. (7).

$$\rho = \frac{\frac{s^2}{12} + \frac{1}{n} \sum_{i=1}^n (y_i - y_b)^2}{(h - y_b) y_b} \quad (7)$$

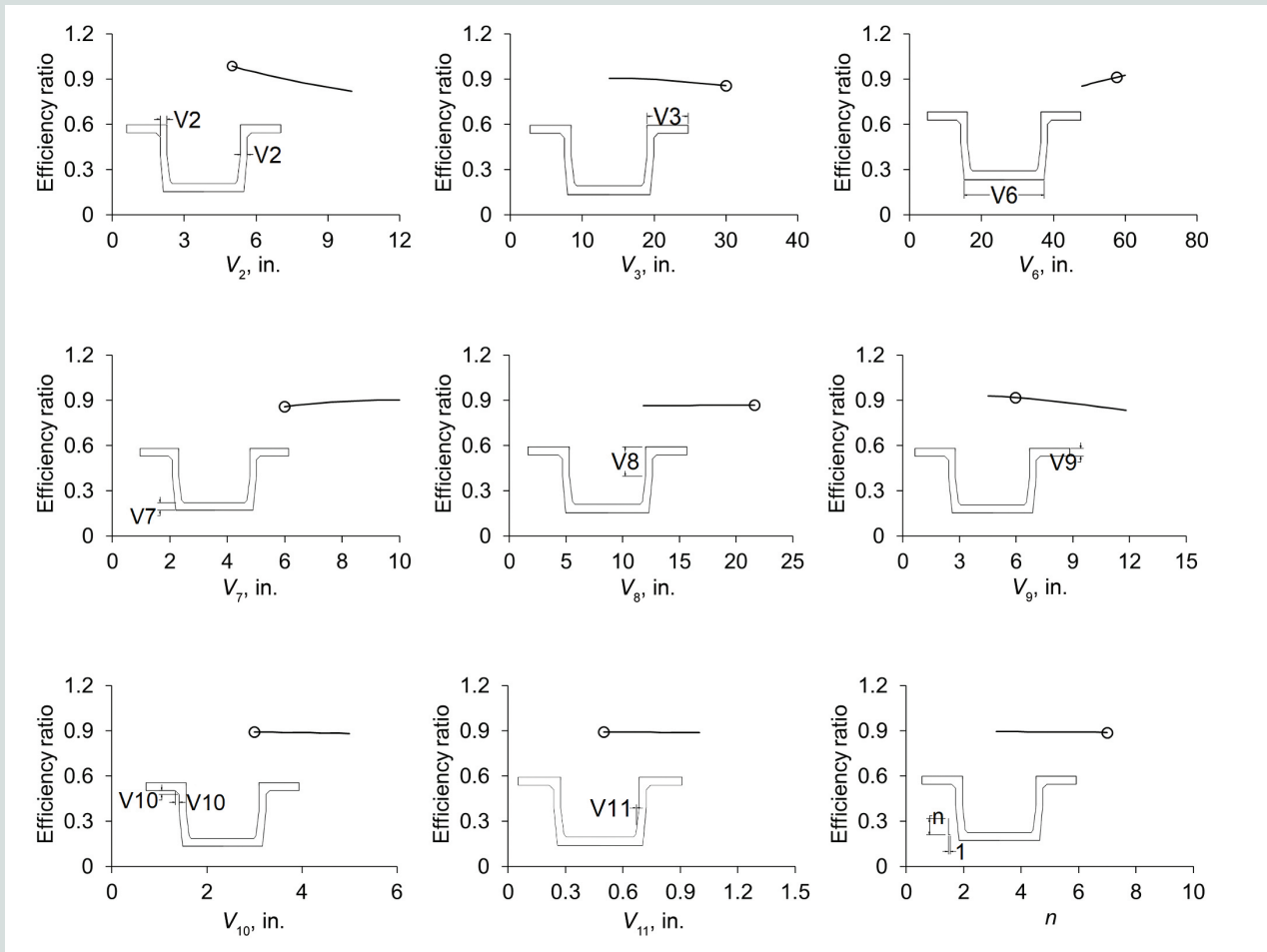


Figure 6. Variation of efficiency ratio with geometric properties (where circle is optimized value). Note: n = number of entities covering the girder section in agent-based modeling; slope of girder web; V_2 = upper web thickness; V_3 = flange length; V_6 = bottom girder width; V_7 = bottom flange thickness; V_8 = depth to web angle; V_9 = upper flange thickness; V_{10} = chamfer; V_{11} = lower web thickness. 1 in. = 25.4 mm.

The portion of the respective entity is calculated using Eq. (8).

$$\rho_i = \frac{\frac{s^2}{12} + (y_i - y_b)^2}{n(h - y_b)y_b} \quad (8)$$

where

ρ_i = efficiency fraction of the i th entity

$$\rho = \sum_{i=1}^n \rho_i w \quad (9)$$

After solving the model, the distribution of the efficiency factors was contoured in color. **Figure 3** describes the contribution of the girder components to the global efficiency factor (Eq. [9]), and the discrepancy between the analytical and computational models was less than 0.41%. The flanges controlled the structural efficiency factors ρ in all cases; by contrast, the web was less influential. This signifies that the dimensions of the flanges and nearby regions (transition from the flanges to the web) can be modified to raise the efficiency of the girders.

Development of prototype tub girders

Optimized section

To enhance the structural efficiency of tub girders in Colorado, the conceptual outline depicted in **Fig. 4** was optimized. The sketch drawn in Fig. 1 was refined with minor modifications, such as haunches and flange cornering, to mitigate stress concentrations. A mathematical algorithm called the generalized reduced gradient (GRG) method was employed to determine the most suitable variables under a given condition. An objective function was defined with the efficiency factor (Eq. [1]) alongside the geometric variables (Fig. 4), and the goal was to maximize the structural efficiency factor ρ . The objective function comprising vectorial components was constrained by upper and lower bounds, as per a possible range taken from the existing state girders (Table 1). Afterward, the function was differentiated with respect to the individual variables to find optimized solutions. The Newton-Rapson method iterated the established procedure until

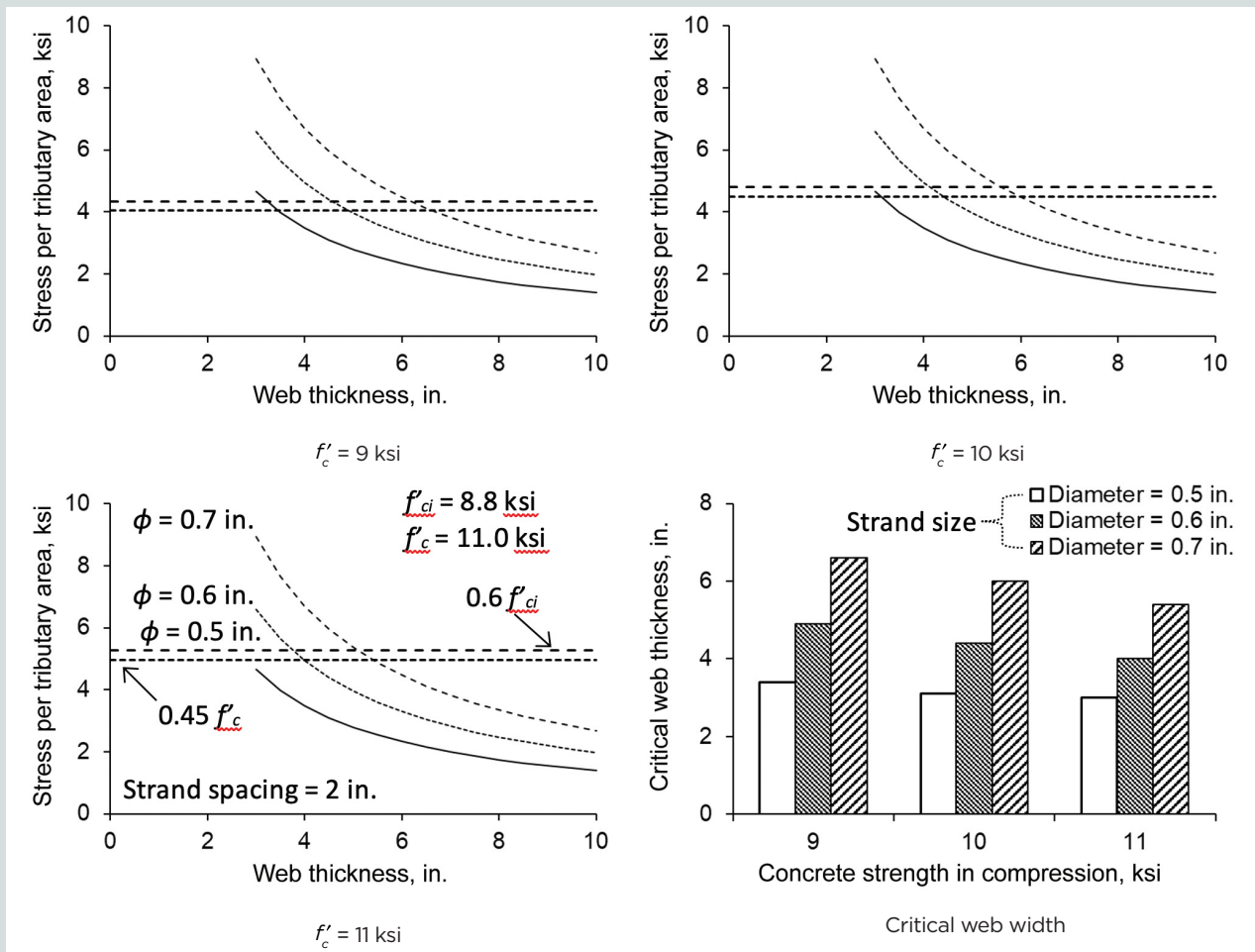


Figure 7. Stress check in the web at transfer against the limit of the American Association of State Highway and Transportation Officials' AASHTO LRFD Bridge Design Specifications (for $f_{pi} = 0.9f_{pj}$). Note: f'_c = specified compressive strength of concrete; f'_{ci} = concrete strength at transfer; f_{pi} = initial stress after transfer; f_{pj} = jacking stress; θ = diameter of steel strands. 1 ksi = 6.895 MPa.

converged values were attained at an estimated difference of 0.0001 between successive gradients. It is worth noting that the gradients of only active constraints were considered to save computational resources. Further details on the GRG algorithm are available elsewhere.¹⁸

Figure 4 shows the optimized section at a depth of 48 in. (1219 mm). Compared with the existing B618 girder (Fig. 1), the straight portion of the webs was increased from 18 to 21.5 in. (457 to 546 mm) (V_8 in Fig. 4) and the width of the bottom flange was enlarged from 54 to 58 in. (1372 to 1473 mm) (V_6 in Fig. 4). **Figures 5 and 6** display the sensitivity of the efficiency factor and ratio with the constituting variables, respectively, and the optimized dimensions were added for a visual appraisal. It should be noted that the primary variables were graphed without the secondary ones (for instance, $V_4 = V_3 - V_2$). When a variable was changed to examine the efficiency of the girder, other variables were kept constant based on the average of the sampled girders (Table 1). For this reason, the optimized values occasionally deviated from the maximum factors and ratios provided in Fig. 5 and 6, respectively. The efficiency factors were more reliant on the

magnitudes of V_2 and V_3 than those of others (Fig. 5), which is ascribed to the fact that the upper flanges of the section dominated the moment of inertia, thereby affecting the radius of gyration in Eq. (1). The variation trend of the efficiency ratio was analogous in general (Fig. 6), whereas the effects of some variables differed owing to the distinct formulation between Eq. (1) and (2).

Web thickness

Because the optimized girder section was solely dependent on its geometric properties, the level of stress in the web where prestressing strands are placed needed to be checked. In line with the web thickness of the existing girders (the Colorado U series in Table 1), a range of web girder thicknesses t_{web} from 5 to 10 in. (127 to 254 mm) were taken into account with strand diameters ϕ of 0.5, 0.6, and 0.7 in. (12.7, 15.2, and 17.8 mm) (with steel strand cross-sectional areas A_p of 0.153, 0.217, and 0.294 in.² [98.7, 140, and 189.7 mm²], respectively). In accordance with the AASHTO LRFD specifications,¹⁴ the specified compressive strengths of the concrete f'_c were 9, 10, and 11 ksi (62, 69, and 76 MPa)

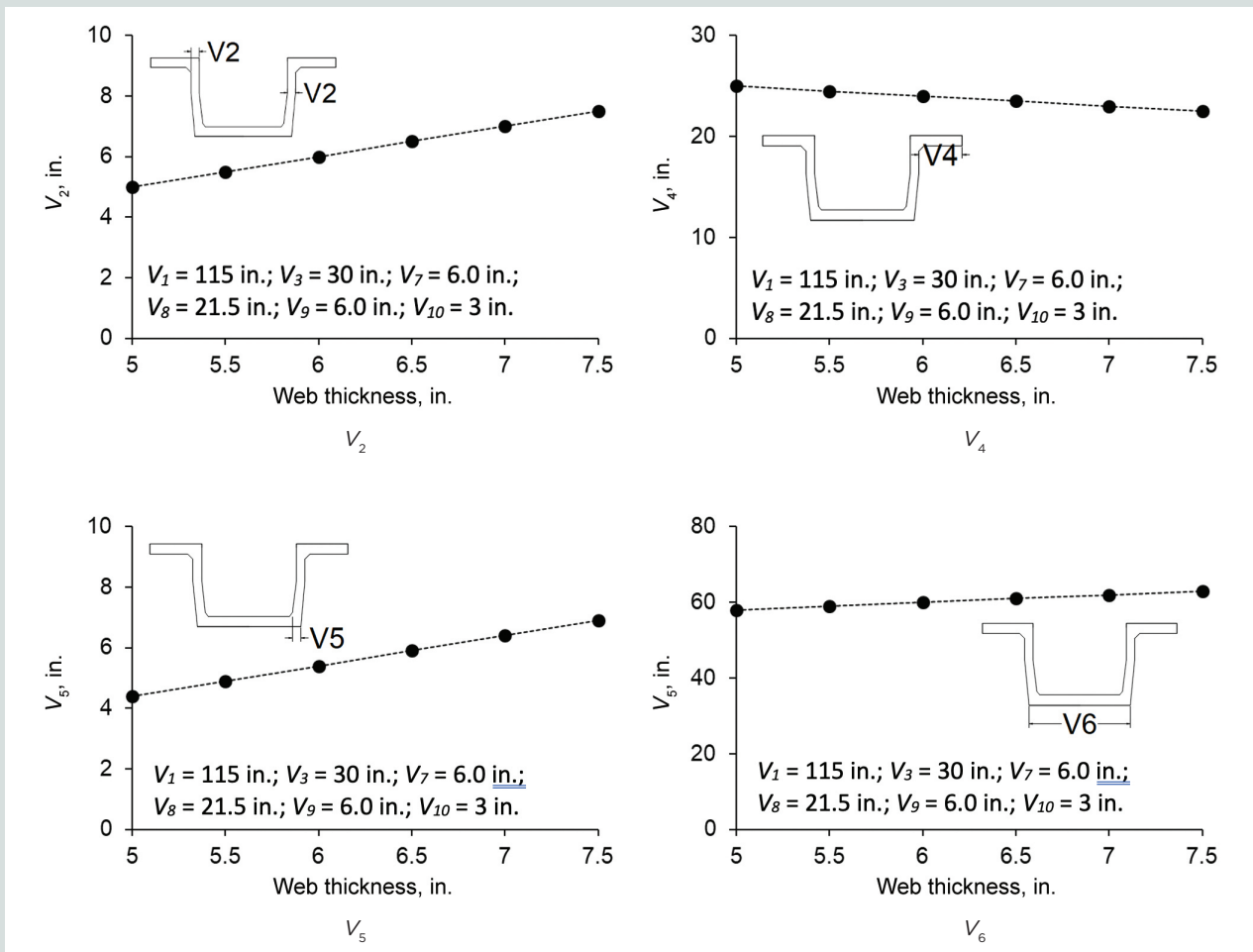


Figure 8. Effects of web thickness on girder geometry (48 in. deep). Note: V_1 = upper girder width; V_2 = upper web thickness; V_3 = flange length; V_4 = flange extension; V_5 = lower web thickness; V_6 = bottom girder width; V_7 = bottom flange thickness; V_8 = depth to web angle; V_9 = upper flange thickness; V_{10} = chamfer. 1 in. = 25.4 mm.

and the strength at transfer was f'_{ci} was $0.8f'_c$. Likewise, the transfer stress of the strands f_i was taken as 90% of the allowable jacking stress of $0.75f_{pu}$ (that is, f_i was $0.675f_{pu}$), where f_{pu} is the ultimate strength of the prestressing steel (270 ksi [1862 MPa]). A tributary area of the web concrete per strand was assumed with a spacing of 2 in. (51 mm), and corresponding stresses were obtained (Fig. 7).

The stress profiles gradually decreased with an increase in the web thickness. The optimized thickness of the girder web t_{web} of 5 in. (127 mm) was acceptable for steel strand diameter ϕ of 0.5 and 0.6 in. (12.7 and 15.2 mm), regardless of concrete strength. In other words, the compressive stress magnitudes induced by the maximum tensioning of the strands were lower than the AASHTO limits of $0.6f'_{ci}$ and $0.45f'_c$ for the compressive stresses before and after losses, respectively. In contrast, the stresses belonging to a steel strand diameter ϕ of 0.7 in. (17.8 mm) were as high as 92.2% relative to its 0.5 in. counterparts. Figure 7 illustrates the critical thickness of the girder web, representing the intersection between the stress profiles and the AASHTO limits in Fig. 7. When the

strand sizes ϕ of 0.5 and 0.6 in. were used, a thickness of 4.9 in. (124.5 mm) was predicted to be sufficient; however, as the strand diameter ϕ was increased to 0.7 in., a thickness of 6.6 in. (167.6 mm) was necessary.

Prototype section

On the basis of the practical significance elaborated before, the optimized section was adjusted to provide multiple options with regard to a web thickness t_{web} of 5 to 7.5 in. (127 to 190.5 mm). The effects of the web thickness are visible in Fig. 8, where invariant geometric properties are indicated. The incremental thickness broadened V_2 (Fig. 8), while it reduced V_4 (Fig. 8) because of the fixed girder width V_1 of 115 in. The response slope of V_5 (Fig. 8) was akin to that of V_2 , which was more susceptible than V_6 (Fig. 8). The proposed dimensions of these adjusted prototype sections were normalized by those of the existing B618 girder (48 in. [1219 mm] deep) (Fig. 9). Except for the vertical portion of the upper web V_8 , all variable ratios associated with the invariant properties were less than unity, meaning that the segments of the proposed

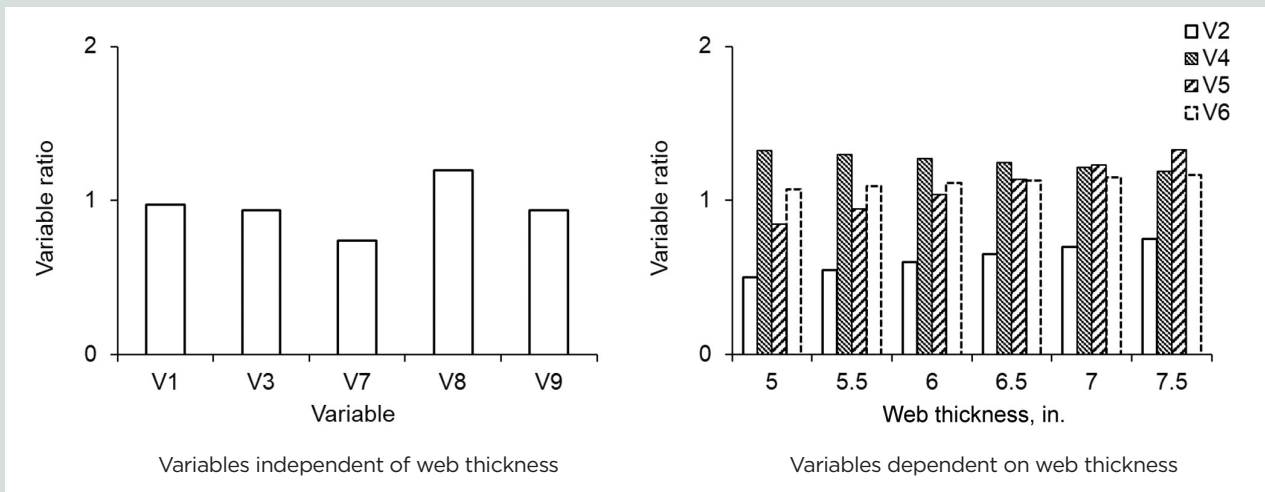


Figure 9. Dimensional analysis of girders at a depth of 48 in. Note: V_1 = upper girder width; V_2 = upper web thickness; V_3 = flange length; V_4 = flange extension; V_5 = lower web thickness; V_6 = bottom girder width; V_7 = bottom flange thickness; V_8 = depth to web angle; V_9 = upper flange thickness. 1 in. = 25.4 mm.

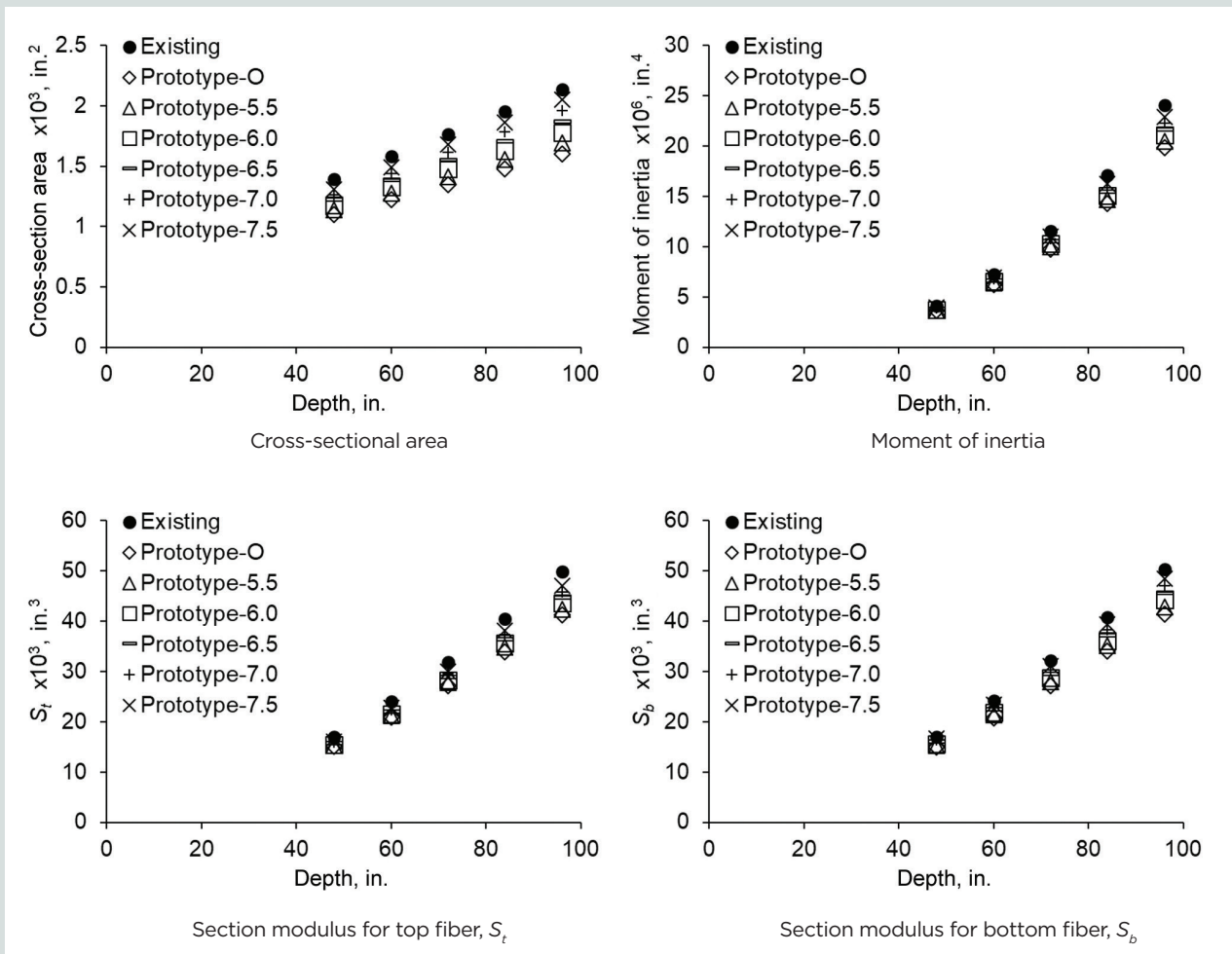


Figure 10. Geometric properties of existing and prototype girders. Note: 1 in. = 25.4 mm; 1 in.² = 645.2 mm²; 1 in.³ = 16,390 mm³; 1 in.⁴ = 416,231 mm⁴.

Table 3. Comparison of structural efficiency between existing Colorado and prototype girders

State/agency	Girder type	Depth, in.	Efficiency factor ρ		Efficiency ratio α		Weight, kip/ft
			Calculated	Normalized*	Calculated	Normalized*	
Colorado DOT	U48	48	0.50	1.00	0.89	1.00	1.43
	U60	60	0.50	1.00	0.89	1.00	1.62
	U72	72	0.50	1.00	0.88	1.00	1.81
	U84	84	0.49	1.00	0.86	1.00	2.01
	U96	96	0.48	1.00	0.85	1.00	2.20
Prototype O	P(O)48	48	0.57	1.14	0.98	1.10	1.14
	P(O)60	60	0.57	1.14	0.98	1.10	1.27
	P(O)72	72	0.56	1.12	0.97	1.10	1.41
	P(O)84	84	0.55	1.12	0.95	1.10	1.54
	P(O)96	96	0.54	1.13	0.93	1.09	1.67
Prototype 5.5	P(5.5)48	48	0.56	1.12	0.97	1.09	1.19
	P(5.5)60	60	0.56	1.12	0.96	1.08	1.33
	P(5.5)72	72	0.55	1.10	0.95	1.08	1.47
	P(5.5)84	84	0.54	1.10	0.93	1.08	1.62
	P(5.5)96	96	0.52	1.08	0.91	1.07	1.76
Prototype 6.0	P(6.0)48	48	0.55	1.10	0.96	1.08	1.23
	P(6.0)60	60	0.54	1.08	0.95	1.07	1.39
	P(6.0)72	72	0.53	1.06	0.93	1.06	1.54
	P(6.0)84	84	0.52	1.06	0.91	1.06	1.70
	P(6.0)96	96	0.51	1.06	0.90	1.06	1.86
Prototype 6.5	P(6.5)48	48	0.54	1.08	0.94	1.06	1.27
	P(6.5)60	60	0.53	1.06	0.93	1.04	1.44
	P(6.5)72	72	0.52	1.04	0.92	1.05	1.61
	P(6.5)84	84	0.51	1.04	0.90	1.05	1.78
	P(6.5)96	96	0.50	1.04	0.88	1.04	1.95
Prototype 7.0	P(7.0)48	48	0.53	1.06	0.93	1.04	1.32
	P(7.0)60	60	0.52	1.04	0.92	1.03	1.50
	P(7.0)72	72	0.51	1.02	0.90	1.02	1.68
	P(7.0)84	84	0.50	1.02	0.88	1.02	1.86
	P(7.0)96	96	0.49	1.02	0.86	1.01	2.04
Prototype 7.5	P(7.5)48	48	0.52	1.04	0.92	1.03	1.36
	P(7.5)60	60	0.52	1.04	0.91	1.02	1.56
	P(7.5)72	72	0.51	1.02	0.89	1.01	1.75
	P(7.5)84	84	0.49	1.00	0.87	1.01	1.94
	P(7.5)96	96	0.48	1.00	0.85	1.00	2.14

Note: DOT = department of transportation; prototype O: optimized section; prototypes 5.5 through 7.5 = adjusted sections.

*Normalized by the value of the existing girder.

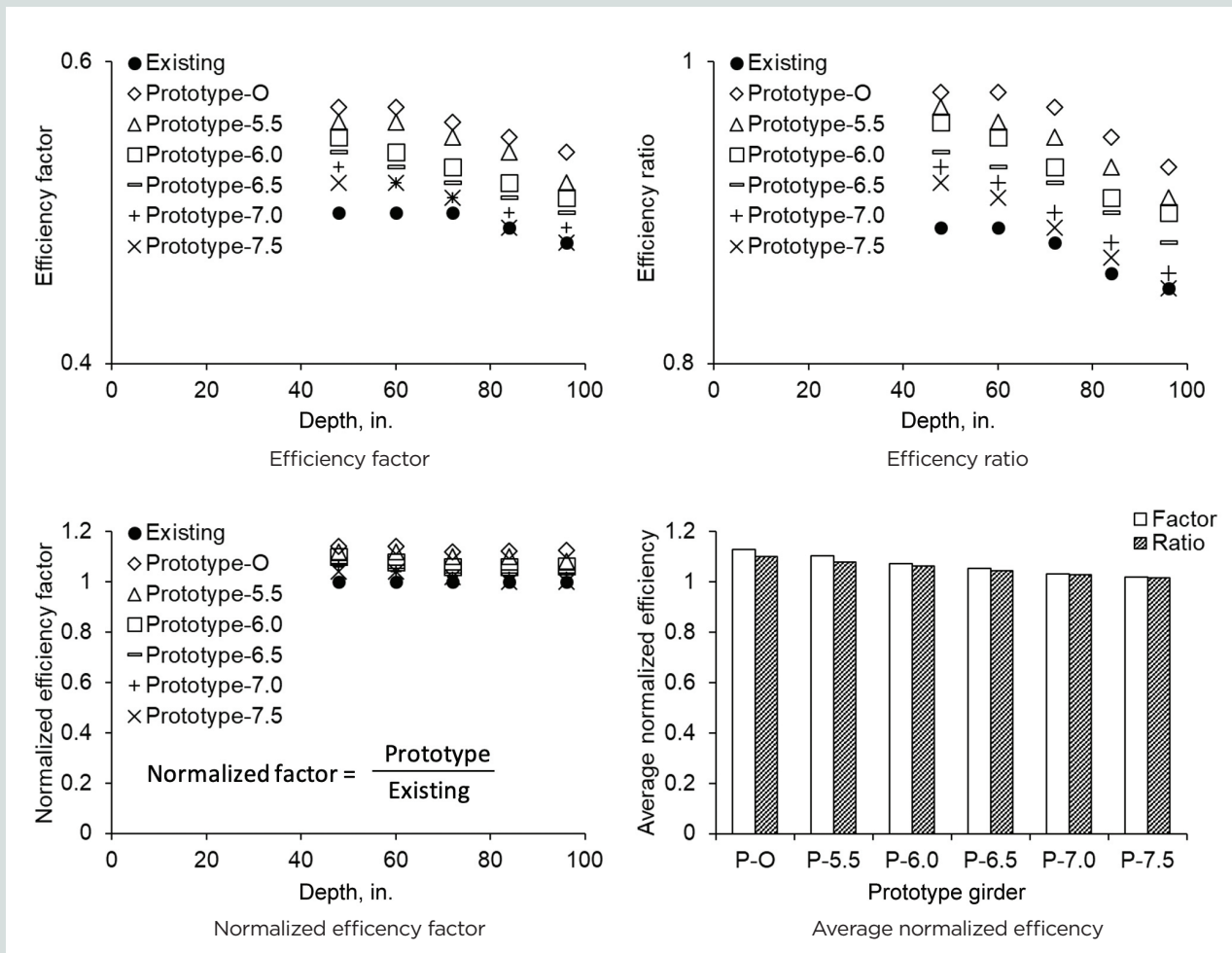


Figure 11. Evaluation of efficiency for existing and prototype girders. Note: 1 in. = 25.4 mm.

prototype section were relatively small and thus a reduction in the self-weight of a new girder series would be expected. Figure 9 reveals the repercussions of other variables related to the web thickness. The intersection between the upper flange and the web V_2 was below a variable ratio of 1.0, at which the proposed and existing dimensions were equal; on the contrary, the lower flange components V_5 and V_6 gradually went up and exceeded the threshold ratio of 1.0 at a web thickness of 6.5 in. (165 mm).

Figure 10 shows the cross-sectional area and the moment of inertia of the tub girders consisting of the aforementioned segmental variables. There was a remarkable gap between the cross-sectional areas of the existing (B618) and optimized (prototype O) girders at a depth of 48 to 96 in. (1219 to 2438 mm), and their difference became reduced with the increased web thickness (prototypes 5.5 to 7.5, representing a thickness of 5.5 to 7.5 in.). As the girder was deepened, the moment of inertia of B618 diverged from that of the prototype sections. The patterns of the section moduli were comparable for the top fibers S_t and bottom fibers S_b in Fig. 10. Since the B618 sections maintained the moduli higher than the

prototype sections, the serviceability of the latter should be checked (to be explained in the “Parametric Investigations” section).

Assessment of efficiency

Table 3 specifies the efficiency of the prototype girders. Irrespective of girder depth, the optimized prototype O sections outperformed the existing B618 sections (**Fig. 11**). Regarding the prototype girders with the adjusted web size (prototypes 5.5 to 7.5), the degree of betterment diminished as the web was widened. This observation is attributed to the fact that, despite the constant neutral axis depth, the increased moment of inertia tended to be offset by the enlarged cross-sectional area in Eq. (1) and (2). The normalized efficiency factors shown in Fig. 11 clarify the structural advantage of the proposed prototype girders; specifically, the efficiency factor and ratio of the tub girders were improved by 12.9% and 10.1%, respectively, on average (Fig. 11). Furthermore, the unit weight of the prototype girders was lowered prominently compared with that of B618 (**Fig. 12**), which would save construction costs by lessening the dead

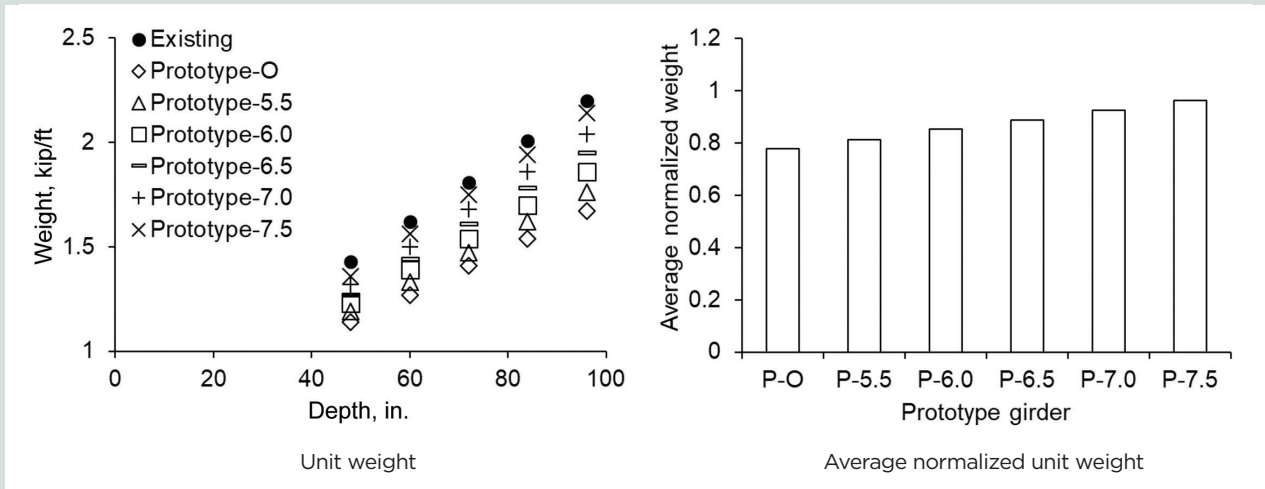


Figure 12. Assessment of prototype girders. Note: 1 in. = 25.4 mm; 1 kip/ft = 14.593 kN/m.

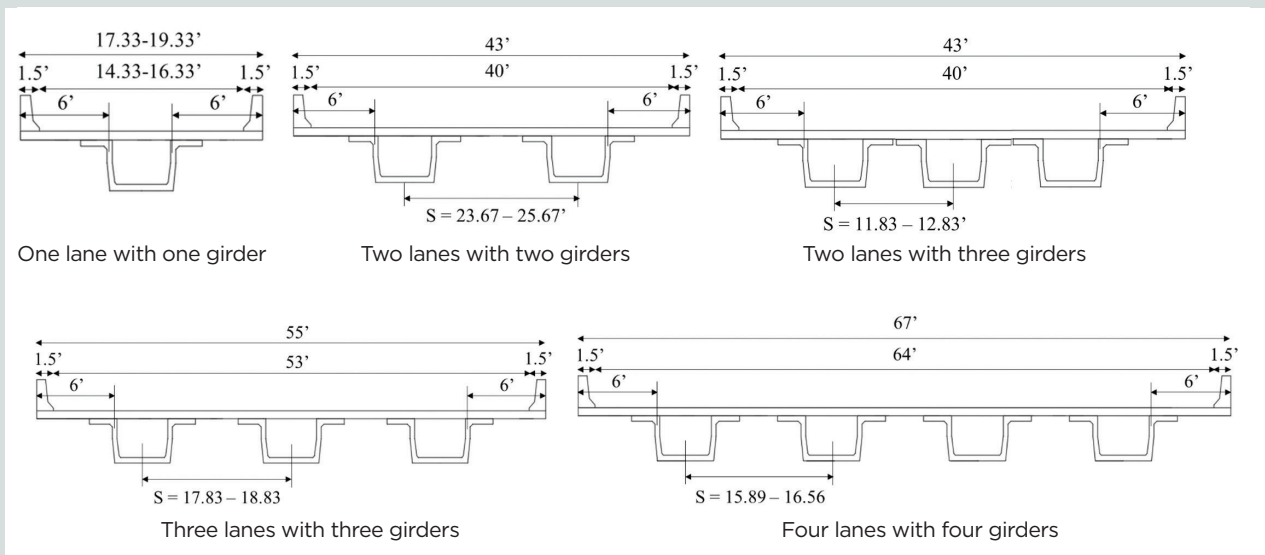


Figure 13. Configuration of superstructure. Note: S = section modulus of girder. 1' = 1 ft = 0.305 m.

load. The extent of an average weight reduction was 22.3% for prototype O and 3.7% for prototype 7.5 (Fig. 12).

Parametric investigations

A parametric study was conducted to examine the compliance of the developed prototype girders with the requirements of AASHTO LRFD bridge design specifications,¹⁴ including serviceability and ultimate limit states. To achieve this aim, five bridge superstructures were designed to accommodate one to four traffic lanes supported by one to four tub girders (Fig. 13). For consistency, an overhang of 6 ft (1.8 m) was commonly used,¹⁹ while the width of shoulders was determined per the AASHTO policy guideline.²⁰ Based on the geometric details of the girders given in Fig. 4 with the variable girder depths from 48 to 96 in. (1219 to 2438 mm)

(Table 3), the maximum achievable spans and associated load effects were calculated. As illustrated in Fig. 14, the prototype girders offered longer spans with almost the same number of steel strands ϕ of 0.6 in. relative to B618. The prototype girders satisfied the serviceability provisions of AASHTO LRFD specifications. (Fig. 15 and 16 display average stresses and deflections taken from the five superstructures.)

Figure 17 summarizes the average responses of the girders. Although the ascending tendency of the factored load effects and flexural capacities of both girders were accompanied by the increased depth, the prototype girders (P series) revealed 6.5% lower capacities in relation to the existing girders (U series), on average, because the former enabled a longer span under the same girder depth as that of the latter. In like manner, the load effects normalized by the maximum spans

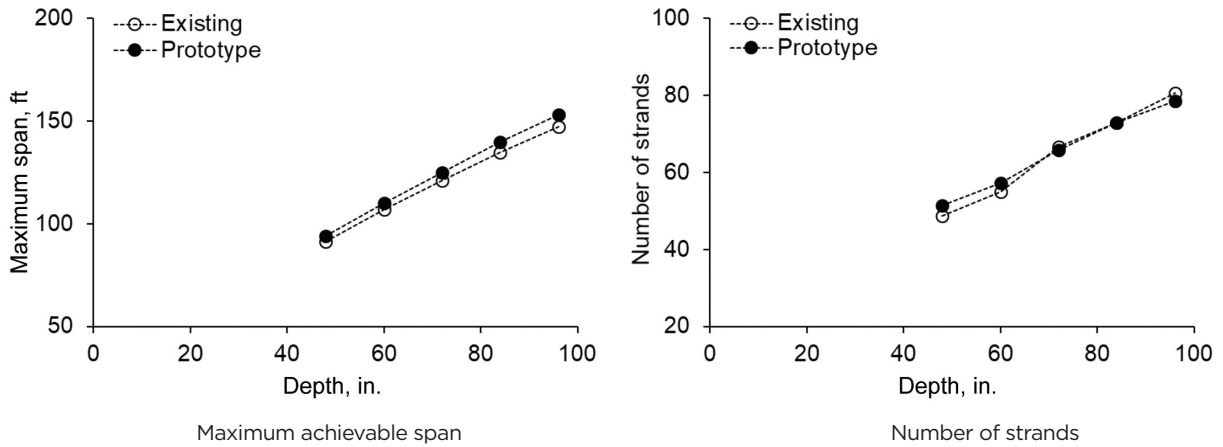


Figure 14. Average configuration of girders. Note: 1 in. = 25.4 mm; 1 ft = 0.305 m.

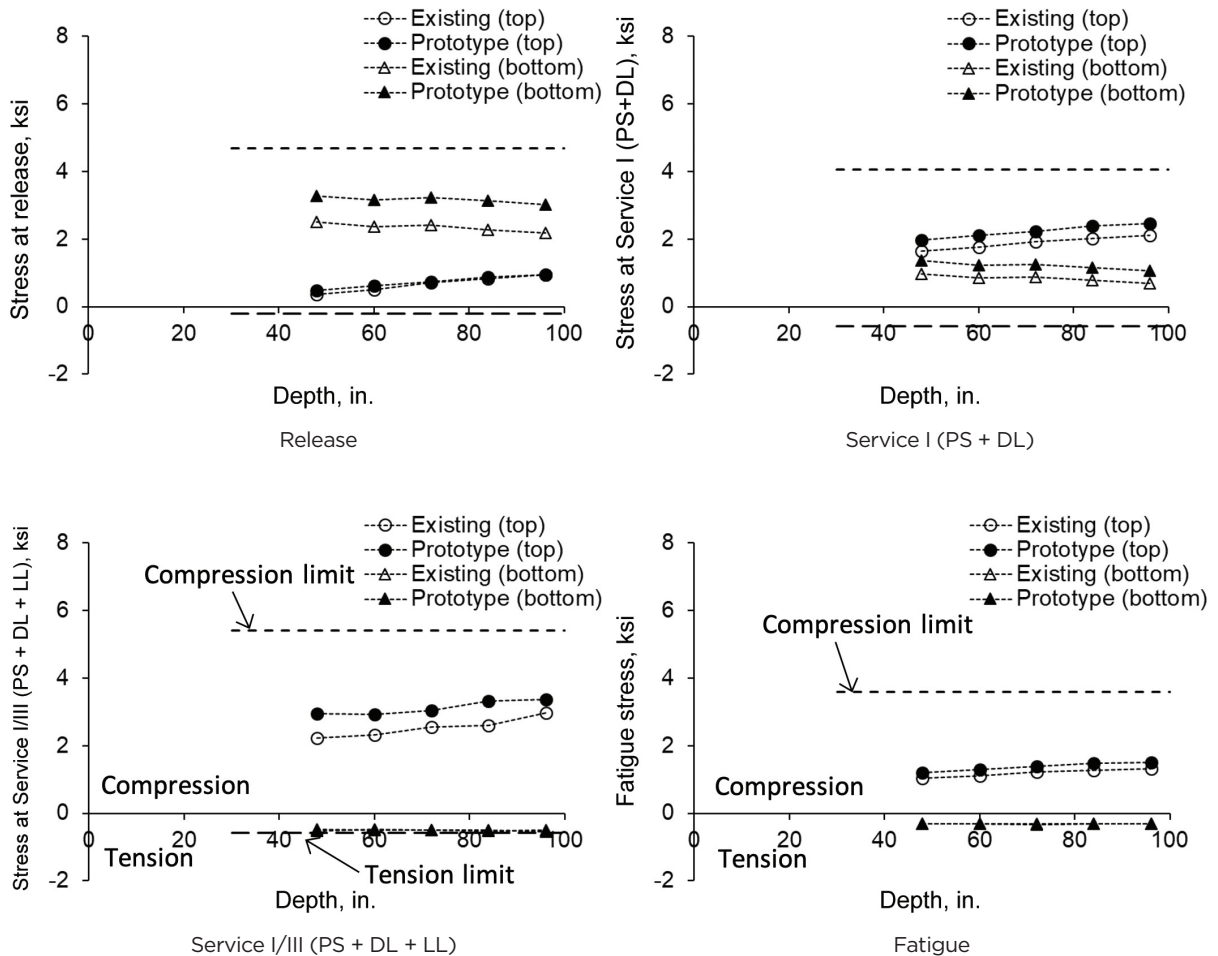


Figure 15. Average stress variation for prototype and existing girders. Note: DL = dead load; LL = live load; PS = prestressed. Note: 1 in. = 25.4 mm; 1 ksi = 6.895 MPa.

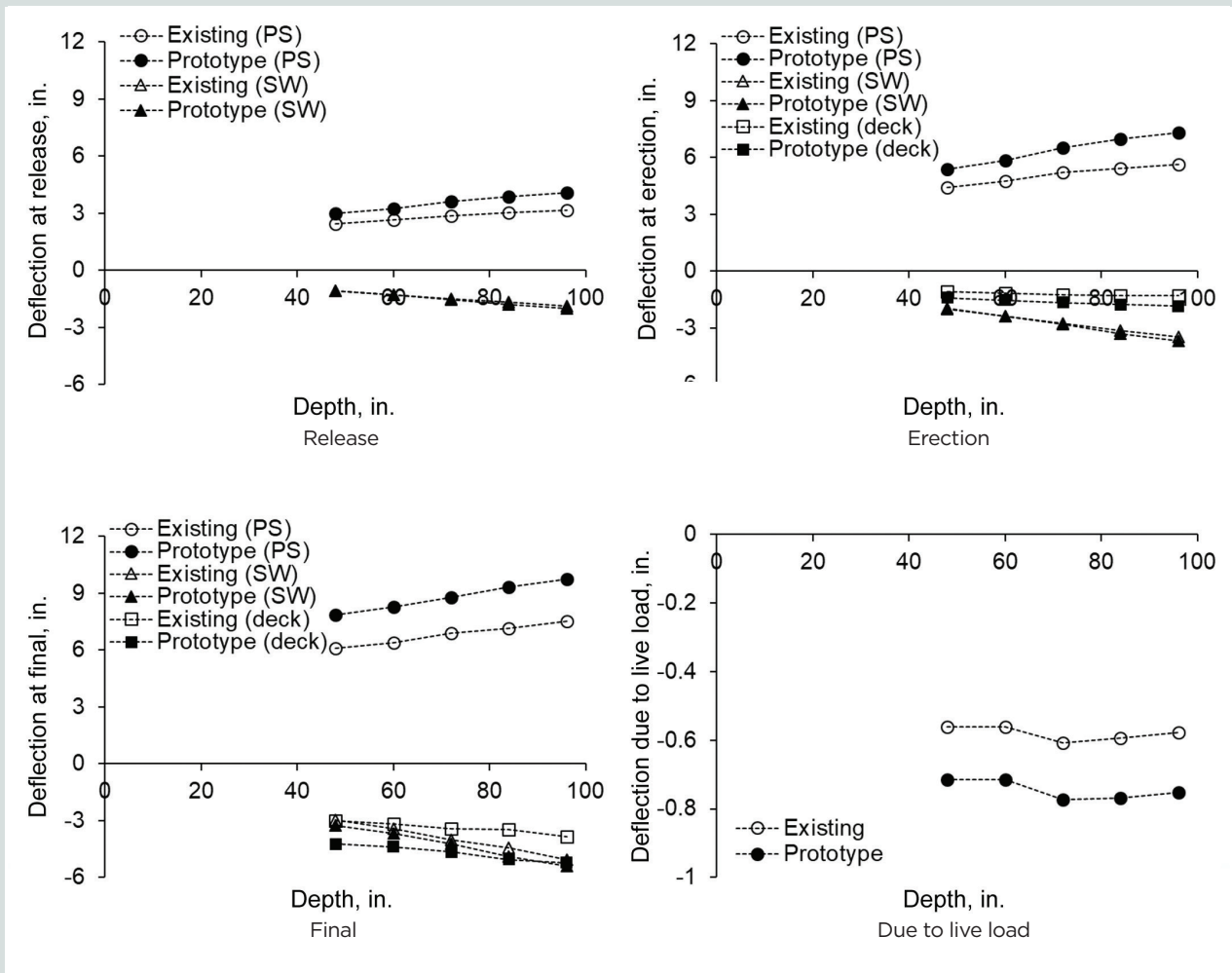


Figure 16. Average deflection for prototype and existing girders. Note: PS = prestressed; SW = self-weight. 1 in. = 25.4 mm.

of the prototype girders were 4.2% lower than the normalized effects of the existing girders. The resistance efficiency of these girder series is shown in Fig. 17, which was obtained by the normalized factored resistance of each section M_R multiplied by its efficiency factor ρ . It is evident that the resistance efficiency of the prototype girders was superior to that of the existing ones, including an average improvement of 10.2%. Concerning the girder capacities normalized by the span, the prototype girders steadily exhibited better performance in terms of the efficiency factor (Fig. 17).

Simplified girder sections considering constructibility

Simplified section

According to the request of the Colorado Department of Transportation, the prototype section was simplified to enhance constructibility. The haunches at the web-flange intersections (V_{10} in Fig. 4) were minimized, and the bilinear exterior webs were changed to straight lines, as in the case of the existing B618 girder. **Figure 18** renders the simplified

version of the prototype girder. Even if these minute adjustments did not alter the structural functionality of the girders, subsidiary tasks were undertaken to elucidate potential concerns about geometric stability.

Buckling analysis

To account for the influence of the revised section, eigenvalue buckling analysis was performed using the commercial finite element analysis package, Ansys. For comparison, the existing, prototype, and simplified configurations were modeled with variable web thicknesses from 5 to 10 in. (127 to 254 mm) along with a segmental length of 3.3 ft (1 m). (Selecting a web size for pre- and post-tensioning is at the discretion of a transportation agency.) Composite sections incorporating a deck slab were not considered because the purpose of the analysis was to examine the relative performance of the three girder types. The elastic modulus E_c and Poisson's ratio ν of the concrete with a concrete compressive strength f'_c of 9000 psi (62 MPa) were 5400 ksi (37,200 MPa) and 0.2, respectively. Three-dimensional concrete elements (SOLID 65) consisting of eight nodes and three degrees of

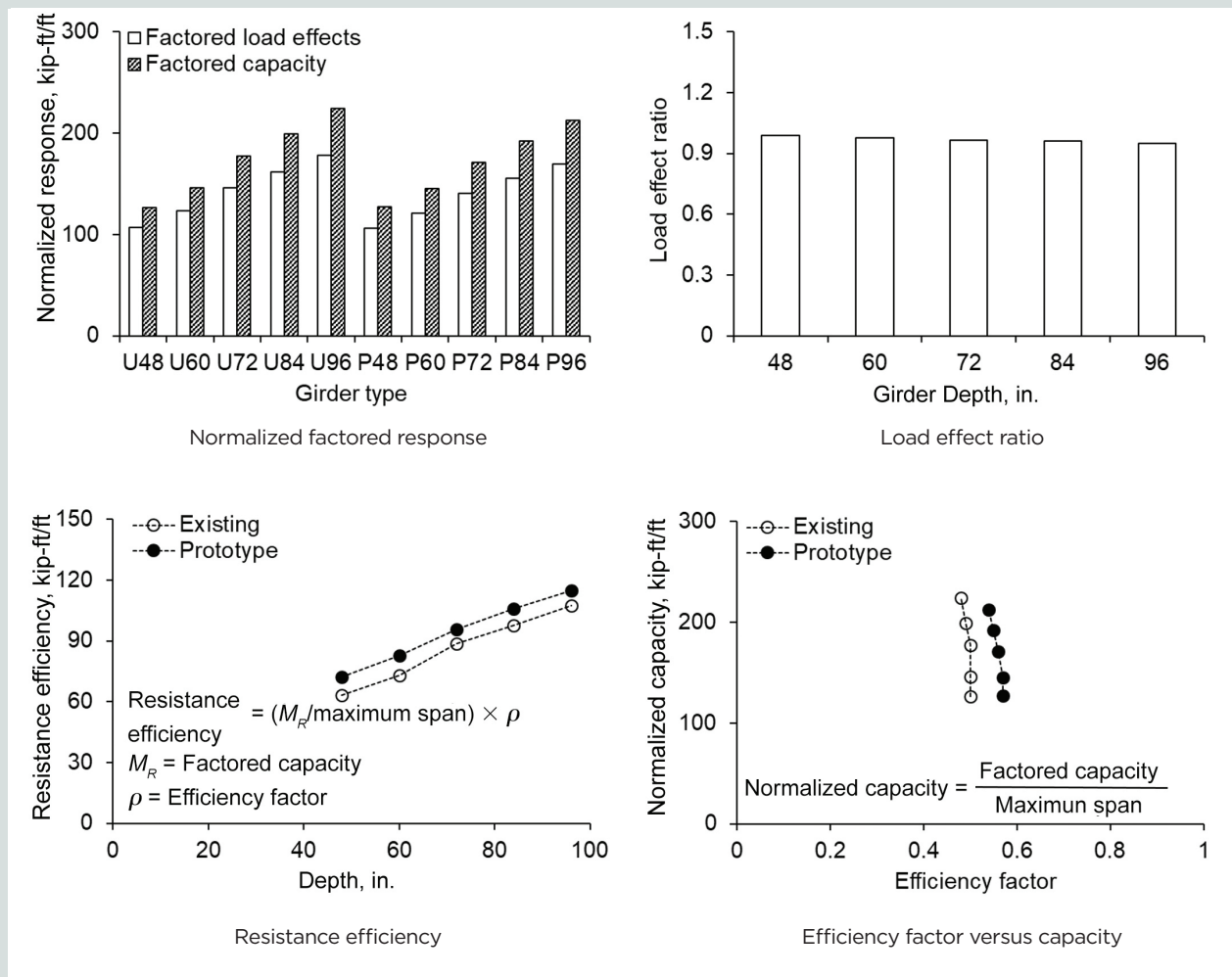


Figure 17. Average response for prototype and existing girders. Note: 1 in. = 25.4 mm; 1 ft = 0.305 m; 1 kip = 4.448 kN.

freedom at a node were formulated to represent the girder shapes (Fig. 19). The steel strands were not included owing to their insignificant contribution to the cross-sectional stiffness of the girders.²¹ The upper flanges of the meshed sections were constrained in the horizontal directions for the presence of a concrete deck in constructed bridges, and the bottom of the sections was fully restrained (in other words, all translational degrees of freedom were fixed as supported by bearing plates in the field). After imposing these boundary conditions, loads were applied on the upper flanges (V_2 in Fig. 4) to compress the webs. Subsequently, the eigenvalues of the sections' first modes were extracted by the Block Lanczos algorithm²² to calculate the buckling load of each girder.

The occurrence of buckling was consistent within the top-third region of the webs throughout the girder shapes and thicknesses. Notwithstanding the similar conformation, the critical loads of the individual sections differed noticeably (Fig. 19). The prototype girders, with web thickness of 5 to 10 in. (127 to 254 mm), buckled at 33,984 to 62,932 kip (151,160 to 279,900 kN). Contrarily, the simplified girders

showed lower loads from 9,121 to 36,464 kip (40,570 to 162,190 kN). For the existing girders where web thicknesses of 5, 7.5, and 10 in. [127, 190.5, and 254 mm] are allowed by the transportation agency, the average buckling load was 13.0% and 65.9% greater than those of the prototype and simplified girders (Fig. 19). Overall, the buckling capacities of the existing and prototype girders were comparable; however, when the simplified girder series is used, internal diaphragms should be placed at support points to address stability issues and deck slabs should be installed on-site to increase the flexural rigidity of the upper flange and restrict the rotations of the flange–web connections and the vulnerable web regions.

Torsional resistance

The torsional rigidity GJ of the sections was appraised to ensure the lateral stability of the girders, where G is the shear modulus of the concrete and J is the section's polar moment of inertia. The shear modulus was gained from elastic theory ($G = E_c / [2(1 + \nu)]$) and the polar moment of inertia was calculated theoretically without using a simplified formula such as the one

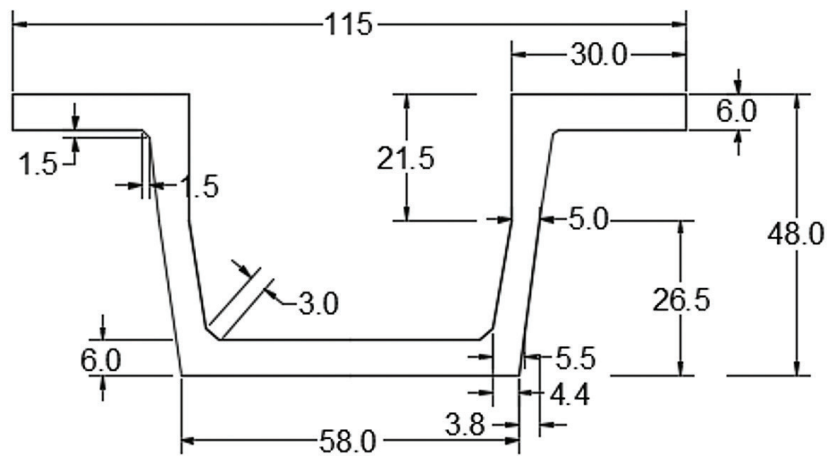


Figure 18. Simplified section for construction convenience. Note: All units are in inches. 1 in. = 25.4 mm.

shown in AASHTO LRFD specifications.¹⁴ The rigidity of the prototype and simplified sections was alike, with an average difference of 1.8%, whereas the response slope of the existing section was lower than that of others (Fig. 20). As such, the torsional performance of the existing section was better at a web thickness of 5 in. (127 mm) (8.37% higher on average), virtually identical at 7.5 in. (190.5 mm), and worse at 10 in. (254 mm) (5.2% lower on average) when compared with the performance of the prototype and simplified sections (Fig. 20). As in the case of the buckling resistance, deck slabs and end diaphragms will alleviate the torsional stress of the girders.

Preliminary cost analysis

Pursuant to the tabulated guidelines of the Florida Department of Transportation,²³ the cost of the three girders was estimated. It is important to note that this section is intended to assess the financial attributes of these girders, rather than provide absolute budgetary information. The one-lane bridge supported by one girder (Fig. 13) was set to the default, which minimized interactions between multiple girders, and the number of steel strands coupled with the depth of the girders mentioned earlier were applied. The average cost of typical tub girders was \$89.10/ft² per unit length with material and labor expenses except for the contribution of manufacturing facilities, equivalent to \$0.59/lb. Figure 21 relates the depth of the prototype girders to projected costs. The cost gap between girder web thickness t_{web} of 5 and 10 in. (127 and 254 mm) increased as the section became deeper. Hence, for pretensioning application, a web thickness t_{web} of 5 in. should first be considered. Similarly, when post-tensioning is planned, a web thickness t_{web} of 7.5 in. (190.5 mm) is suggested unless a web thickness t_{web} of 10 in. is imperative for structural reasons. Figure 21 shows the average costs of the three girder types. The B618 girders were 4.2% and 2.4% more expensive than the prototype and simplified girders per foot, respectively. If a span of 150 ft (46 m) is to be designed with the prototype and

simplified girders, the owner may save more than \$6108 and \$3566, respectively, per girder.

Conclusion

This paper explores the development of new prestressed concrete tub girders in Colorado. To begin with, the strengths and weaknesses of existing state girders (35 types reviewed from 6 transportation agencies across the United States) were evaluated. Analytical and computational approaches were then utilized to quantify the structural efficiency of CDOT's B618 series. Through a mathematical algorithm, an optimized girder section was identified and its practical significance was appraised with a strand diameter ϕ of 0.5, 0.6, and 0.7 in. (12.7, 15.2, and 17.8 mm) at a compressive concrete strength f'_c of 9, 10, and 11 ksi (62, 69, and 76 MPa). The applicability of proposed prototype girders was investigated in the context of AASHTO LRFD bridge design specifications¹⁴ covering the serviceability and ultimate limit states. To comprehend the practicality of the prototype girders, five bridge superstructures were designed and their behavior was studied. The prototype sections were simplified for the sake of constructability by modifying haunches and bilinear exterior web lines. The production costs of the girders were estimated and monetary benefits were discussed for the prototype and simplified girders. Although the behavior of the girders in shear was not examined, adequate shear reinforcement can readily address strength requirements. The following conclusions are drawn:

- Among the existing tub girders, the Texas and Florida specimens showed higher efficiency than others. The unit weight of the Colorado girders was heavier, which could unfavorably raise the dead load of a bridge system. Accordingly, the weight of B618 was recommended to be lowered to meet the range of the Florida and Washington girders.

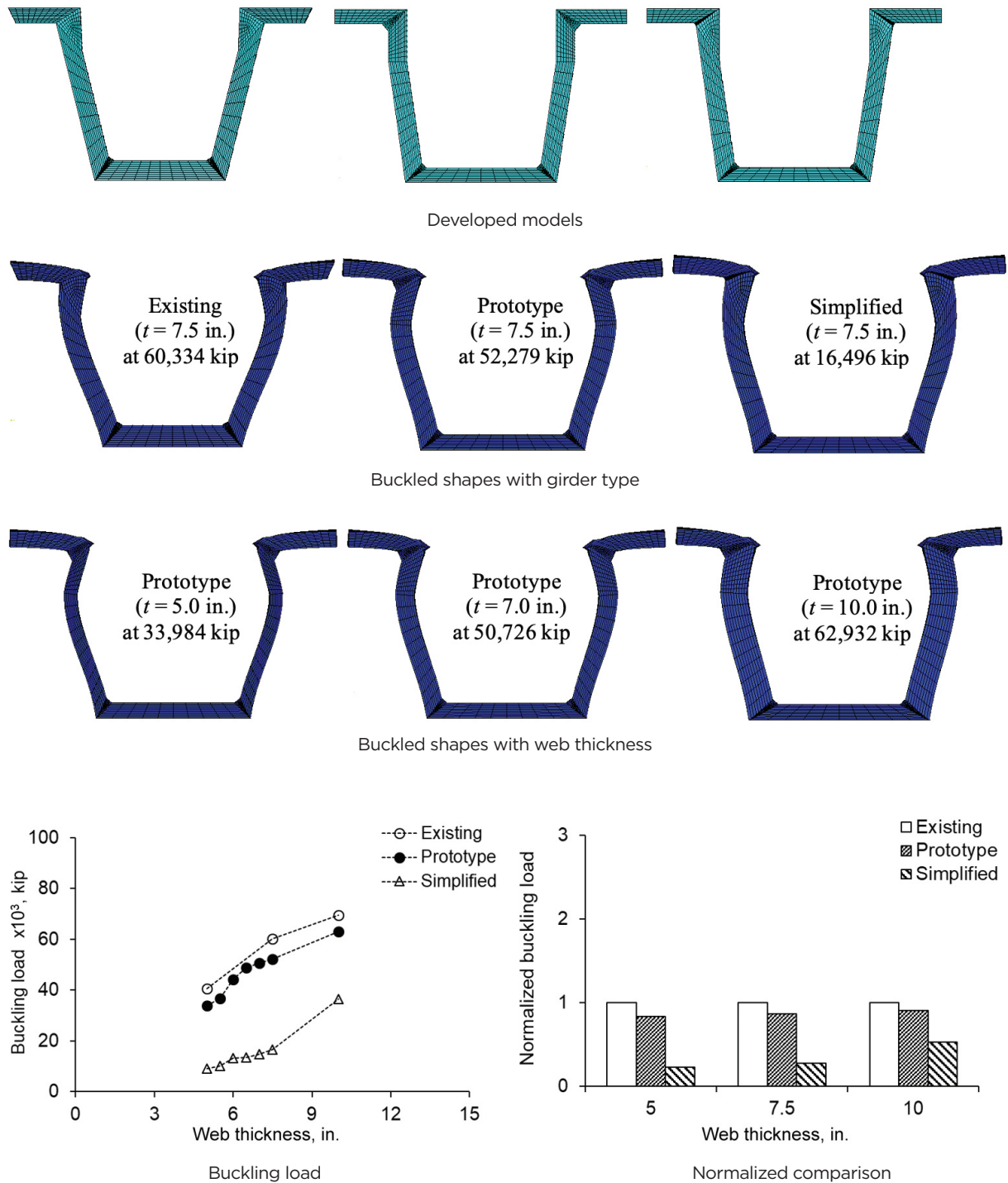


Figure 19. Buckling of tub girders at a depth of 72 in. Note: t = web thickness. 1 in. = 25.4 mm; 1 kip = 4.448 kN.

- Relative to the B618 girders, the optimized section enhanced the efficiency by up to 12.9%, with a reduction in unit weight (kip/ft) as low as 22.3%. The 5 in. (127 mm) web thickness of the prototype girder with a strand diameter ϕ of 0.5 and 0.6 in. (12.7 and 15.2 mm) maintained compressive stress levels below the limits of AASHTO LRFD specifications, while a wider web thickness t_{web} of 6.6 in. (167.6 mm) was necessary for a strand diameter ϕ of 0.7 in. (17.8 mm).
- Parametric analysis of the one- to four-lane superstructures indicated that the prototype girders enabled longer spans and greater resistance efficiency compared with the B618 girders without increasing the

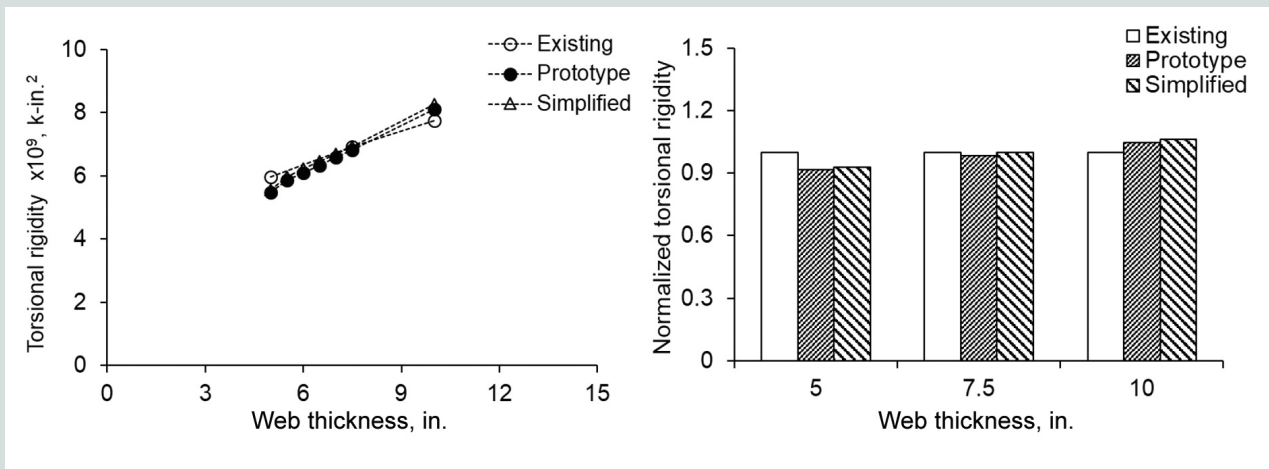


Figure 20. Torsional resistance of girders at a depth of 72 in. Note: 1 in. = 25.4 mm; 1 kip-in.² = 2870 kN-mm².

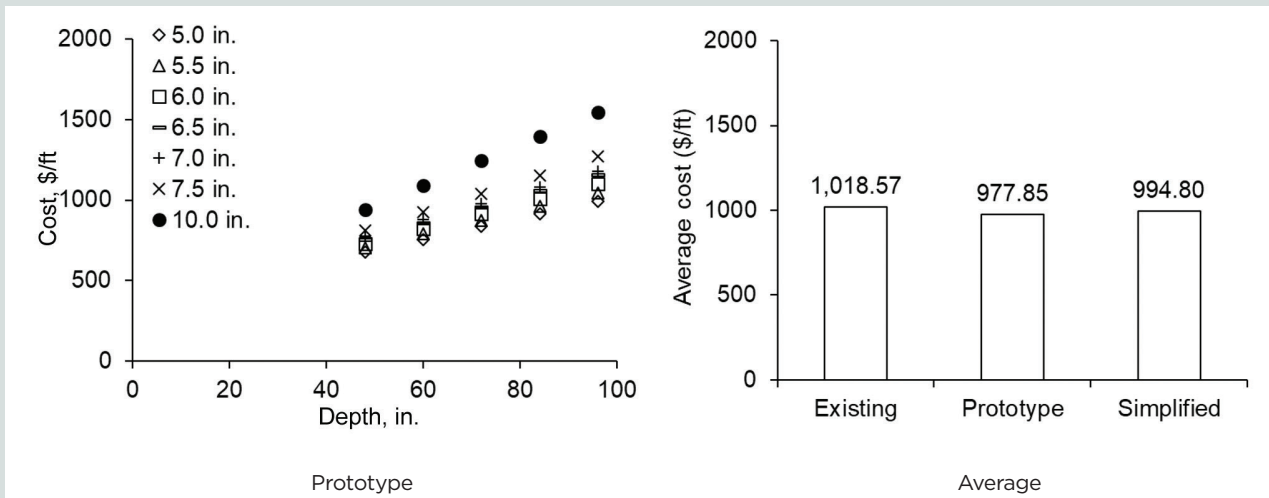


Figure 21. Cost estimate. Note: 1 in. = 25.4 mm; 1 ft = 0.305 m.

number of steel strands.

- The buckling-critical zone of all tub girders was located within the top third region of the webs. The buckling load of the prototype with a web thickness t_{web} of 5 to 10 in. (127 to 254 mm) was tantamount to that of B618, while the stability of the simplified sections did not reach those levels and the use of bracing elements was recommended. On the torsional rigidity of these three girders, there was no notable difference.
- In compliance with the relationship between the cost gap and web thickness, t_{web} of 5 and 7.5 in. (127 and 190.5 mm) should first be considered for pretensioned and post-tensioned girders, respectively. The costs of the existing girders were 4.2% and 2.4% higher than those of the prototype and simplified girders per foot, respectively.

Acknowledgments

The authors gratefully acknowledge support from the Colorado Department of Transportation (CDOT). T. Tran and T. Wang were the research manager and the lead panel, respectively, who advised this project. The contents of this paper reflect the views of the authors and do not necessarily reflect the official views of CDOT or any other agencies.

References

1. Pipinato, A. 2022. *Innovative Bridge Design Handbook: Construction, Rehabilitation and Maintenance*. 2nd ed. Cambridge, MA: Butterworth-Heinemann, Elsevier.
2. Nawy, E. G. 2010. *Prestressed Concrete: A Fundamental Approach*. Upper Saddle River, NJ: Prentice Hall.

3. Benaim, R. 2019. *The Design of Prestressed Concrete Bridges: Concepts and Principles*. Boca Raton, FL: CRC Press.
4. Bardow, A. K., R. L. Seraderian, and M. P. Culmo. 1997. "Design, Fabrication and Construction of the New England Bulb-Tee Girder." *PCI Journal* 42 (6): 30–40. <https://doi.org/10.15554/pcij.11011997.30.40>.
5. Seguirant, S. J. 1998. "New Deep WSDOT Standard Sections Extend Spans of Prestressed Concrete Girders." *PCI Journal* 43 (4): 92–119. <https://doi.org/10.15554/pcij.07011998.92.119>.
6. Hovell, C., A. Avendano, A. Moore, D. Dunkman, O. Bayrak, and J. Jirsa. 2013. *Structural Performance of Texas U-beams at Prestress Transfer and under Shear-Critical Loads*. Report FHWA/TX-13/0-5831-2. Austin, TX: Center for Transportation Research.
7. Amir, O., and E. Shakour. 2018. "Simultaneous Shape and Topology Optimization of Prestressed Concrete Beams." *Structural and Multidisciplinary Optimization*, no. 57, 1831–1843.
8. Saindon, K. C., and M. L. McMullen. 2010. "Curved Precast Prestressed Concrete Bridge Girder Systems." In *Structures Congress 2010*, 51–58. Reston, VA: American Society of Civil Engineers.
9. Ralls, M. L., L. Ybanez, and J. J. Panak. 1993. "The New Texas U-beam Bridges: An Aesthetic and Economical Design Solution." *PCI Journal* 38 (5): 20–29. <https://doi.org/10.15554/pcij.09011993.20.29>.
10. Huang, D. and Shahawy, M. 2005. "Analysis of Tensile Stresses in Transfer Zone of Prestressed Concrete U-beams." *Transportation Research Record*, no. 1928, 134–141.
11. Reese, G.A. 2010. "Innovative Applications of Precast Concrete to Complex Bridge Projects in Colorado." *Transportation Research Record*, no. 2200, 154–159.
12. Marti, J. V., F. Gonzalez-Vidosa, V. Yepes, J. Alcala. 2013. "Design of Prestressed Concrete Precast Road Bridges with Hybrid Simulated Annealing." *Engineering Structures*, no. 48, 342–352.
13. Alawneh, M., M. K. Tadros, and C. Sun. 2022. "Optimized Ultra-high-performance Concrete Horizontally Curved Bridge Superstructure." *PCI Journal* 67 (2): 34–54.
14. AASHTO (American Association of State Highway and Transportation Officials). 2020. *AASHTO LRFD Bridge Design Specifications*. 9th ed. Washington, DC: AASHTO.
15. Rabbat, B. G., and H. G. Russell. 1982. "Optimized Sections for Precast Prestressed Bridge Girders." *PCI Journal* 27 (4): 88–104. <https://doi.org/10.15554/pcij.07011982.88.106>.
16. FDOT (Florida Department of Transportation). 2020. *Index 450-210 Series Florida-U beams*. Tallahassee, FL: FDOT.
17. Wilensky, U., and W. Rand. 2015. *An Introduction to Agent-based Modeling*. Boston, MA: The MIT Press.
18. Lasdon, L. S., R. L. Fox, and M. W. Ratner. 1973. *Nonlinear Optimization Using the Generalized Reduced Gradient Method*. Technical Memorandum 325. Springfield, VA: National Technical Information Service, U.S. Department of Commerce.
19. CDOT (Colorado Department of Transportation). 2012. *Bridge Design Manual*. Denver, CO: CDOT.
20. AASHTO. 2018. *A Policy on Geometric Design of Highways and Streets*. 7th ed. Washington, DC: AASHTO.
21. Okumus, P., M. G. Oliva, and S. Becker. 2012. "Nonlinear Finite Element Modeling of Cracking at Ends of Pretensioned Bridge Girders." *Engineering Structures*, no. 40, 267–275.
22. Saini, H. S., R. Sayal, A. Govardhan, and R. Buyya. 2021. *Innovations in Computer Science and Engineering*. Singapore: Springer Nature.
23. FDOT. 2022. *Bridge Development Report Cost Estimate*. Tallahassee, FL: FDOT. <https://www.fdot.gov/docs/default-source/structures/structuresmanual/currentrelease/bdrbridgecostestimate.xlsx>.

Notation

A	= cross-sectional area
A_p	= cross-sectional area of steel strands
E_c	= elastic modulus of concrete
G	= shear modulus of concrete
H	= girder depth
f'_c	= specified compressive strength of concrete
f'_{ci}	= concrete strength at transfer
f_i	= transfer stress of strands
f_{pi}	= initial stress after transfer

f_{pj}	= jacking stress	ν	= Poisson's ratio
f_{pu}	= ultimate strength of prestressing steel	ρ	= structural efficiency factor
I	= moment of inertia	ρ_i	= efficiency fraction of i th entity in agent-based modeling
M_R	= factored resistance of girder section	ϕ	= diameter of steel strands
n	= number of entities covering the girder section in agent-based modeling; slope of girder web		
r	= radius of gyration		
s	= width and depth of entity in agent-based modeling		
S	= section moduli of girder		
S_b	= section modulus for bottom fiber		
t_{web}	= thickness of girder web		
ν	= Poisson's ratio		
V	= geometric parameter		
V_1	= upper girder width		
V_2	= upper web thickness		
V_3	= flange length		
V_4	= flange extension		
V_5	= lower web thickness		
V_6	= bottom girder width		
V_7	= bottom flange thickness		
V_8	= depth to web angle		
V_9	= upper flange thickness		
V_{10}	= chamfer		
V_{11}	= lower web thickness		
y_b	= distance from centroid of girder section to bottom fiber of girder		
y_i	= distance from girder bottom to centroid of i th entity in agent-based modeling		
y_t	= distance from centroid of girder section to top fiber of girder		
α	= structural efficiency ratio		

About the authors



Yail J. Kim, Ph.D, P.Eng., F.ACI, is president of the Bridge Engineering Institute, an international technical society, and a professor in the department of civil engineering at the University of Colorado Denver. His research

interests encompass advanced composite materials for rehabilitation, structural informatics, complex systems, and science-based structural engineering, including statistical, interfacial, and quantum physics.



Jun Wang is a postdoctoral fellow in the department of civil engineering at the University of Colorado Denver. Her research interest include multiobject interaction, concrete structures, and advanced computational simulations.

Abstract

This paper presents a new tub girder series for Colorado, conforming to the articles of the American Association of State Highway and Transportation Officials' *AASHTO LRFD Bridge Design Specifications*. Although the B618 tub girders developed by the Colorado Department of Transportation in the 1990s have been successfully used for decades, the need for an upgrade is essential to satisfy the requirements of contemporary bridge design and construction. After examining the performance of tub girders selected from six transportation agencies in the United States, an optimization algorithm was employed to generate efficient prototype sections. Then, detailed investigations were conducted to examine various practical aspects concerning the serviceability and ultimate limit states of AASHTO LRFD specifications. Parametric analysis with five bridge superstructures that accommodate up to four traffic lanes demonstrated the applicability of the prototype girders. A simplified version of the prototype sections was also delineated for regional precasters. Furthermore, a comparative study was carried out to evaluate the geometric stability and production costs of the prototype, simplified, and existing B618 girders.

Keywords

Bridge, development, load and resistance factor design, LRFD, prestressed concrete, tub girder.

Review policy

This paper was reviewed in accordance with the Precast/Prestressed Concrete Institute's peer-review process. The Precast/Prestressed Concrete Institute is not responsible for statements made by authors of papers in *PCI Journal*. No payment is offered.

Publishing details

This paper appears in *PCI Journal* (ISSN 0887-9672) V. 69, No. 2, March–April 2024, and can be found at <https://doi.org/10.15554/pcij69.2-01>. *PCI Journal* is published bimonthly by the Precast/Prestressed Concrete Institute, 8770 W. Bryn Mawr Ave., Suite 1150, Chicago, IL 60631. Copyright © 2024, Precast/Prestressed Concrete Institute.

Reader comments

Please address any reader comments to *PCI Journal* editor-in-chief Tom Klemens at tklemens@pci.org or Precast/Prestressed Concrete Institute, c/o *PCI Journal*, 8770 W. Bryn Mawr Ave., Suite 1150, Chicago, IL 60631. 